ASSESSING THE ROLE OF URBAN FOREST STRUCTURE IN CARBON SEQUESTRATION OF BEIJING, CHINA

MURTAZA, A.[1] – MUSHTAQ, P.[1] – XU, C. Y.[1] – DHUNGANA, K.[2] – ZHANG, X. N.[1*] – ULLAH, S.[3*]

[1]Research Center for Urban Forestry of Beijing Forestry University, Key Laboratory for Silviculture and Forest Ecosystem of State Forestry and Grassland Administration, The Key Laboratory for Silviculture and Conservation of Ministry of Education, Beijing Forestry University, Beijing 100083, China

[2]Ministry of Forest and Environment, Gandaki Province 33700, Nepal

[3]Department of Water Resources and Environmental Engineering, Nangarhar University, Jalalabad 2600, Nangarhar, Afghanistan

[*]Corresponding authors
e-mail: zhangxinna0513@163.com; sajidjalwan@gmail.com

(Received 12th May 2025; accepted 10th Jul 2025)

Abstract. Urbanization and climate change are global challenges, with cities contributing significantly to carbon emissions. Urban Forests (UF) mitigate climate change by sequestering carbon, but their potential depends on structural complexity and diversity. However, the relationship between UF structure and carbon storage remains poorly understood, particularly in rapidly urbanizing regions like Beijing. This study investigates how structural attributes of urban forests (UF) in Beijing, China, influence carbon density in biomass and soil. The structural attributes considered include species diversity, diameter and height class diversity, and stand structure. The aim of which is to optimize carbon sequestration through tailored management. Using Generalized Additive Models (GAMs), the study analyzed non-linear relationships between structural factors and carbon density. Both biomass and soil carbon dynamics were evaluated. Greater species and structural diversity, particularly in diameter and height classes, significantly increased biomass carbon density. Forests with heterogeneous structures showed greater carbon storage capacity. Larger tree metrics, such as average diameter at breast height (DBH), strongly correlated with both biomass and soil carbon density. Stand structure had minimal impact on soil carbon, which was more influenced by tree height and DBH. The GAMs demonstrated high predictive accuracy, with an adjusted R^2 of 0.912 and 94.2% deviance explained. The study highlights the importance of structural complexity in UF for enhancing carbon sequestration. It recommends prioritizing the cultivation and conservation of larger trees, which significantly contribute to carbon storage. The use of GAMs offers a robust predictive tool for urban forestry management, providing actionable insights for policymakers and urban planners to optimize carbon storage and mitigate climate change impacts.
Keywords: *biomass, generalized additive models (GAMs), structural diversity*

Introduction

Over half of the world's population resides in urban areas, a figure projected to increase to 68 % by 2050 (He et al., 2021; Guo et al., 2024; Ullah et al., 2024b, 2025a). Cities are major contributors to climate change (Ullah et al., 2024a, c, 2025b), accounting for a significant share of global carbon dioxide (CO_2) emissions due to concentrated energy consumption, transportation, and industrial activities (Sarkodie et al., 2020; Wu et al., 2025a; Yu et al., 2025). To mitigate these impacts, cities must adopt sustainable development strategies, including enhancing carbon sequestration through urban greenspaces (Sun et al., 2019; Shadman et al., 2022, Du et al., 2024). Urban forests (UF) play a critical role in this regard, offering multifaceted benefits such as reducing the urban

http://www.aloki.hu ● ISSN 1589 1623 (Print) ● ISSN1785 0037 (Online)
DOI: http://dx.doi.org/10.15666/aeer/2305_85678605

heat island (UHI) effect (Vogt et al., 2017; Zürcher and Andreucci, 2017), improving air quality (Escobedo et al., 2008; Bottalico et al., 2016), and providing recreational spaces (Chen et al., 2018; Chen and Li, 2021). However, rapid urbanization and densification policies often prioritize development over green infrastructure (Gelan and Girma, 2021; Brom et al., 2023), threatening the functionality of UF and their ability to deliver ecosystem services (Zhang, 2025; Li, T. & Li. Y., 2023).

Despite their importance, the economic and ecological value of UF remains undervalued due to limited public awareness and challenges in quantifying their contributions (Nowak et al., 2018). While urban trees and forests are recognized for their climate-regulating services, such as carbon sequestration (Oberle et al., 2023; Ganesh and Pragasan, 2022), the mechanisms driving carbon storage in UF are poorly understood (Scholz et al., 2018; Giraldo-Charria et al., 2025). Previous studies have focused on isolated locations or specific subpopulations, such as trees in urban parks (Georgi and Zafiriadis, 2006; Yang et al., 2025), rather than addressing UF as a whole (Morgenroth et al., 2020). Additionally, the relationship between structural diversity such as species richness, diameter, and height class diversity and carbon storage remains unclear, particularly in rapidly urbanizing regions like Beijing. This gap hinders the development of effective management strategies to optimize carbon sequestration in urban ecosystems.

This study aims to investigate the structural attributes of UF in Beijing and their implications for carbon stock modeling. Specifically, it seeks to (1) examine how species diversity, diameter and height class diversity, and stand structure influence carbon density in biomass and soil, and (2) develop predictive models using Generalized Additive Models (GAMs) to capture non-linear relationships between structural factors and carbon storage. Understanding the role of structural complexity in UF is critical for enhancing carbon sequestration and mitigating climate change impacts. This study provides actionable insights for urban planners and policymakers, offering a scientifically grounded approach to optimize carbon storage in urban ecosystems. By integrating advanced modeling techniques, such as GAMs, the research also contributes to the development of predictive tools for sustainable UF management. Ultimately, this work underscores the importance of prioritizing structural diversity in urban forestry practices to maximize carbon sequestration and resilience in the face of global environmental challenges.

Material and methods

Study area

Beijing, located in northern China on the North China Plain, Beijing (115.7° to 117.4° E, 39.4° to 41.6° N) spans a total area of 16,410.54 km² (*Fig. 1*). Beijing is one of the world's oldest cities, has undergone rapid urbanization in recent decades, making it an ideal case study for this research. From 1984 to 2008, Beijing's urbanized area expanded 3.4 times, accompanied by a 53.4% increase in the number of permanent residents (Mao et al., 2014). The city's diverse land uses include residential areas (52.64%), woodlands (7.04%), institutional zones (6.83%), industrial and commercial districts (4.62%), transportation networks (2.91%), and other categories (Yan et al., 2020). This combination of rapid urbanization and varied land-use patterns provides a unique opportunity to explore the structural properties of urban forests (UF) and their role in carbon stock modeling. According to the study of Zhang et al. (2024), which analyzed the spatiotemporal dynamics of urban expansion in Beijing, the China Urban Planning

http://www.aloki.hu ● ISSN 1589 1623 (Print) ● ISSN1785 0037 (Online)
DOI: http://dx.doi.org/10.15666/aeer/2305_85678605

and Design Research Institute determined an urban expansion elasticity coefficient of 1.12. From 1995 to 2020, the urban construction land area in Beijing's core urban zones increased by 53%, with varying rates of expansion. The construction land area slightly declined by 2% from 1995 to 2000, then grew by 8% from 2000 to 2005, followed by a significant 29% increase from 2005 to 2010. Growth slowed thereafter, with an 8% expansion from 2010 to 2015 and a 3% increase from 2015 to 2020, reflecting a pattern of "contraction, slow growth, medium growth, slow growth (Zhang et al., 2024). The interplay between Beijing's rich historical heritage, fast-paced urban development, and diverse land uses creates a compelling context for investigating how UF structural attributes influence carbon sequestration and inform sustainable urban planning strategies.

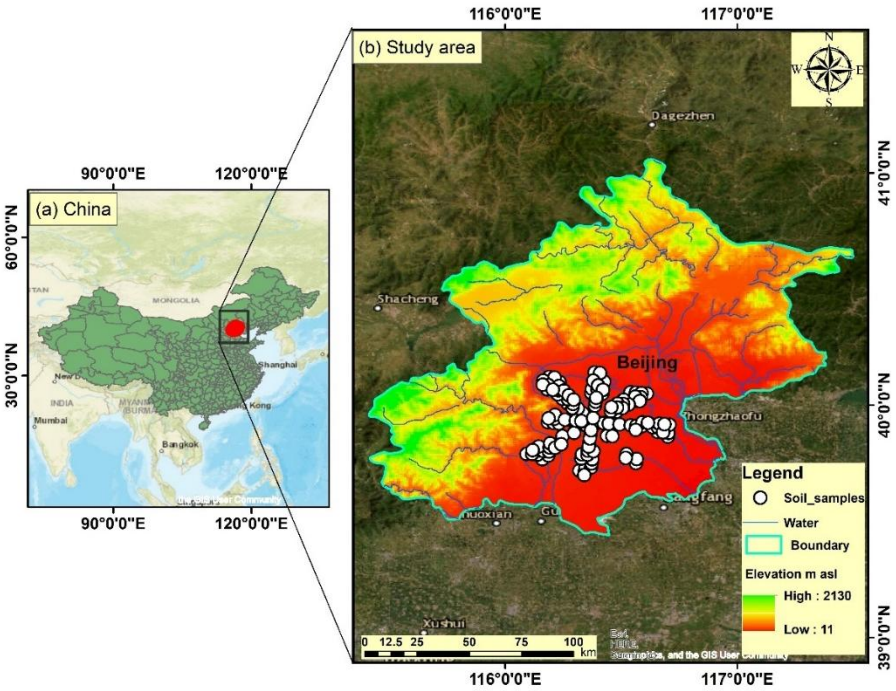

Figure 1. *Location map of the study area: Beijing, China*

Sampling design

The inventory design for this study encompassed boundary mapping, plot layout, and detailed measurements of trees, saplings, leaf litter, herbs, and grasses. A total of 157 square plots, each measuring 30 m × 30 m, were established using a systematic sampling approach (Bhuyan, 2003). In this method, sample plots are arranged in a regular pattern, often along lines or grids, to ensure even coverage of the study area. Systematic sampling is particularly effective for large or heterogeneous regions, as it captures the spatial variability of the ecosystem. For this study, sample plots were distributed across 8 triangular arcs radiating from the center of the study area, with plots systematically arranged along lines within each arc. These plots were strategically distributed across Beijing's urban landscape, capturing variations in proximity to infrastructure, tree species composition, and forest age. Additionally, 147 soil samples were collected from the same plots to assess soil characteristics. Surface soil (0–20 cm) was collected using the "five-point" sampling method in each plot. This involved removing surface litter and humus,

http://www.aloki.hu ● ISSN 1589 1623 (Print) ● ISSN1785 0037 (Online)
DOI: http://dx.doi.org/10.15666/aeer/2305_85678605

and then collecting five soil samples from each plot, which were fully mixed into one composite sample (Li et al., 2022). The composite soil samples were air-dried and then passed through a sieve for further analysis. Soil organic carbon was calculated with these soil samples (Wu et al., 2025b). To ensure a comprehensive assessment of vegetation layers, nested subplots of 2 m × 2 m and 1 m × 1 m were established within each main plot, positioned in all four corners. This nested design enabled detailed measurements of herbs and shrubs, providing a holistic evaluation of the forest's structural attributes.

Data collection and field measurements

Field data collection was conducted from September to November 2023. During this period, measurements of tree height, diameter at breast height (DBH), and under-branch height were recorded for all trees with a DBH greater than 4 cm within the sample plots. DBH was measured by diameter tape to the nearest millimeter.

Trees with a DBH less than 4 cm were excluded from measurements, as they contributed minimally to the aboveground biomass (AGB) in the forests (Obonyo et al., 2023). For each woody plant with a DBH > 4 cm, the following data were collected: Species identification, number of trees per species, tree height, DBH, health condition, canopy coverage estimation, crown density recording, and presence of pests or signs of disease (*Figure 2*). Tree height was measured using abney's level, canopy density was measured using densitometer.

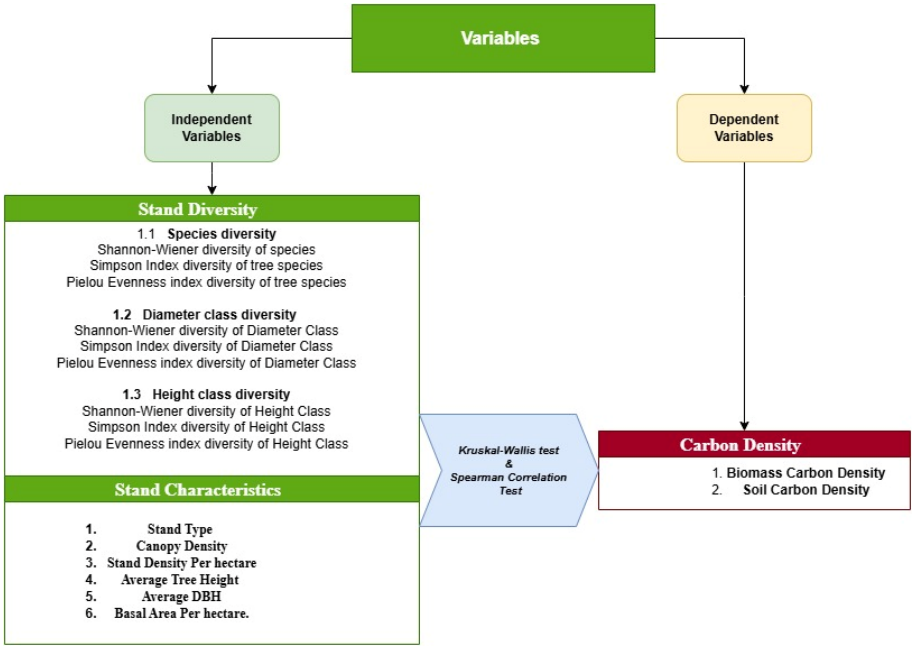

Figure 2. *Variables used in this study*

DBH, one of the most commonly measured tree structural attributes, was prioritized due to its ease of measurement and strong correlation with both structural and non-structural urban forest characteristics (Morgenroth et al., 2020). The position of each plot center was recorded with an accuracy of 2 meters, along with site location data and structural characteristics such as crown height, canopy cover, branching patterns, and evidence of pests (He et al., 2025). A total of 147 soil samples were collected from the

http://www.aloki.hu ● ISSN 1589 1623 (Print) ● ISSN1785 0037 (Online)
DOI: http://dx.doi.org/10.15666/aeer/2305_85678605

same plots used for tree measurements. Soil samples were obtained using a soil corer and auger to collect both undisturbed and disturbed samples for bulk density and soil organic carbon (SOC) analysis, respectively. The five-point sampling method was employed to collect surface soil (0–20 cm depth) from each plot. Surface litter and humus were removed before collecting five subsamples per plot, which were thoroughly mixed to form a composite sample (Li et al., 2022). The composite samples were air-dried and sieved for subsequent analysis.

Structural attributes and diversity indices

Structural attributes and diversity indices were calculated to quantify species richness, evenness, and heterogeneity within the sample plots. The following indices were used:

Species diversity

Shannon-Wiener index (H) (Ortiz-Burgos, 2016)

Measures species diversity by accounting for both abundance and evenness using *Equation 1*.

$$H = -\Sigma p_i \cdot \ln (p_i) \quad \text{(Eq.1)}$$

where:
H = Shannon Diversity Index,
p_i = proportion of individuals of species i in the entire community,
Σ = sum symbol,
ln = natural logarithm
Higher values indicate greater diversity.

Simpson's index (D) (Simpson, 1949):

Measures the probability that two randomly selected individuals belong to the same species using *Equation 2*.

$$D = \frac{\Sigma n_i(n_i-1)}{N(N-1)} \quad \text{(Eq.2)}$$

where:
D = Simpson's Index (ranges from 0 to 1; 0 = infinite diversity, 1 = no diversity),
ni = number of individuals of species i,
N = total number of individuals.
Simpson's Index of Diversity (1 - D) (Zhao et al., 2025b): Represents the probability of two individuals belonging to different species. Higher values indicate greater diversity.

*Pielou's evenness index (J') (*Pielou,1966)

Quantifies how evenly individuals are distributed among species. For this purpose, we have used *Equation 3*.

$$J' = -\frac{\Sigma p_i \ln (p_i)}{\ln (S)} \quad \text{(Eq.3)}$$

http://www.aloki.hu ● ISSN 1589 1623 (Print) ● ISSN1785 0037 (Online)
DOI: http://dx.doi.org/10.15666/aeer/2305_85678605

where:
J′ = Pielou's Evenness Index,
S = total number of species.

Margalef's richness index (R) (Thakural, 2017)

Measures species richness, accounting for the number of species and individuals using *Equation 4*.

$$R = \frac{S-1}{\ln(N)} \quad \text{(Eq.4)}$$

where:
R = Margalef's Richness Index,
S = total number of species,
N = total number of individuals.

Berger-Parker index (Berger et al., 1970)

The Berger-Parker diversity index measures the dominance of the most abundant species using *Equation 5*.

$$d = \frac{N_{max}}{N} \quad \text{(Eq.5)}$$

where:
R = Berger-Parker Index,
N_{max} =Count of the most abundant species,
N = total number of individuals across all species.

Importance value index (IVI)

Assesses species dominance by combining relative density, relative frequency, and relative dominance using *Equation 6*.

$$IVI = Relative\ Density + Relative\ Frequency + Relative\ Dominance \quad \text{(Eq.6)}$$

Diameter and height complexity

Diameter classes were divided into 4 cm intervals, starting from 4 cm, while height classes were divided into 2 m intervals. These metrics provide a comprehensive understanding of structural diversity and distribution patterns in the urban forest.

Shannon-Wiener Index: This index quantifies the diversity and evenness of diameter and height distributions within the plots. Shannon-Wiener Index applied to diameter and height classes to measure Diameter Heterogeneity (DH) and Height Heterogeneity (HH).

Simpson Index: This index evaluates the probability of two randomly selected individuals belonging to the same diameter or height class. Simpson Index was used to diameter and height classes to measure Diameter Distribution Evenness (DD) and Height Distribution Evenness (HD).

http://www.aloki.hu ● ISSN 1589 1623 (Print) ● ISSN1785 0037 (Online)
DOI: http://dx.doi.org/10.15666/aeer/2305_85678605

Pielou Evenness Index: This index assesses how evenly individuals are distributed across diameter and height classes. Pielou Evenness Index was applied to diameter and height classes to measure Evenness of Diameter Distribution (DE and Evenness of Height Distribution (HE).

Stand structure

Stand structure was characterized using several key attributes: A categorical variable including Broadleaf Pure Forest, Evergreen Mixed Forest, Evergreen Pure Forest, Mixed Forest, and Plantation. The proportion of the forest floor covered by the vertical projection of tree crowns, measured using a densiometer (0% = no canopy, 100% = dense canopy). This metric provides insights into light penetration and the forest's microclimate. The number of trees per hectare (trees/ha), calculated by extrapolating tree counts from sample plots. This metric helps assess tree population density and resource competition. The mean height of trees within the sample plots. The mean diameter at breast height of trees within the sample plots. The total cross-sectional area of all trees at breast height, expressed in m^2/ha. This metric reflects forest density and productive potential. These structural attributes were analyzed to evaluate their effects on urban forest carbon density and their contribution to ecosystem services.

Soil carbon calculation

Soil carbon content was calculated using undisturbed soil cores to estimate bulk density. The cores were dried at 105°C to a constant weight, and the soil mass per unit volume (g/cm^3) was determined by dividing the weight by the core volume. Soil carbon content was derived by multiplying the soil organic carbon (SOC) percentage by the bulk density, converting the SOC fraction into mass per unit volume (mg C/cm^3). Soil carbon density was then calculated by multiplying the soil carbon content by the soil layer depth, allowing the expression of soil carbon in units of g C/m^2 for a prescribed depth. This integrated method provides accurate measurements of soil carbon and insights into the carbon storage potential of urban forests (Qiu et al., 2023; Zhao et al., 2025a).

Calculation of biomass and carbon stock

Tree biomass and carbon stocks were estimated using allometric equations, a non-destructive method based on biophysical variables such as diameter at breast height (DBH), tree height, and wood density. Biomass for each tree was calculated using species-specific allometric equations from the "China's Normalized Tree Biomass Equation Dataset" (Luo, 2018). Carbon storage in above-ground biomass (AGB) and below-ground biomass (roots) was calculated using *Equation 7*.

$$\text{Biomass Carbon} = \text{Total Biomass} * C\% \quad \text{(Eq.7)}$$

where:
C% is the carbon conversion factor. A carbon factor of 0.47 was applied to AGB (IPPC, 2006).

Statistical analysis

GAMs were used to model non-linear relationships between structural attributes (e.g., species diversity, diameter/height class diversity, stand characteristics) and carbon

http://www.aloki.hu ● ISSN 1589 1623 (Print) ● ISSN1785 0037 (Online)
DOI: http://dx.doi.org/10.15666/aeer/2305_85678605

density. GAMs were implemented in R (R Core Team, 2024) using the mgcv package (Wood, 2017). we employed Generalized Additive Models (GAMs), a versatile statistical modeling technique, to investigate the combined effects of various ecological diversity indices and stand characteristics on carbon density. GAMs are a flexible and powerful class of statistical models that allow us to explore potential nonlinear relationships between predictor variables and a response variable, in this case, the biomass carbon density of certain tree species. Unlike linear models, GAMs can capture non-linear patterns by combining multiple smooth functions of predictor variables. GAMs are particularly valuable when investigating intricate dependencies, making them a crucial tool for data analysis and predictive modeling.

The analysis was performed using the mgcv package in R, which is specifically designed for fitting generalized additive models. The model was constructed with carbon density as the dependent variable, while incorporating smooth functions of various predictor variables, including diversity indices according to species diversity, diameter class diversity, and height class diversity. The diversity indices used were the Shannon-Wiener diversity of species, Simpson Index diversity of tree species, Pielou Evenness index diversity of tree species, Shannon-Wiener diversity of diameter classes within the plot, Simpson Index diversity of diameter classes, Pielou Evenness index diversity of diameter classes, Shannon-Wiener diversity of height classes within the plot, Simpson Index diversity of height classes, and Pielou Evenness index diversity of height classes. Predictors for stand characteristics included Stand Type, Canopy Density, Stand Density Per hectare, Average Tree Height, Average DBH, and Basal Area Per hectare.

The model formulation employed spline smoothing terms for continuous variables, allowing us to capture non-linear trends in the data. Additionally, categorical variables such as Stand Type were included as factors in the model. The fitting process was completed using the gam () function from the mgcv library, followed by model diagnostics and evaluation of the predictive performance and residuals (Sun et al., 2025).

ANOVA and T test were performed to examine the variance of Biomass and carbon among different plots and to find the correlation between structural characteristics and total biomass. Pearson correlation and linear regression were used to assess relationships between structural attributes (e.g., DBH, height) and biomass. Furthermore; Kruskal-Wallis and Spearman's rank correlation were employed to evaluate associations between structural attributes and carbon density.

Results

Species diversity in the urban forest

The urban forest surveyed in this study comprised 2,517 trees from 65 species and 31 families. Broad-leaved species dominated the landscape, accounting for 84% of the total tree population, while conifers represented 16%. Among these, 75% were deciduous species, and the remaining 25% were evergreen. The most abundant family was Rosaceae, with 13 species, followed by Salicaceae (8 species) and Pinaceae (6 species). This composition reflects a diverse and ecologically rich urban forest, with a mix of species adapted to varying environmental conditions.

To quantify species diversity, several indices were calculated. The Shannon-Wiener Index value of 3.231 indicates high species diversity, reflecting both richness (number of species) and evenness (distribution of individuals among species) (*Table 1*). Similarly, the Simpson's Diversity Index (D) value of 0.056 suggests low dominance by any single

http://www.aloki.hu ● ISSN 1589 1623 (Print) ● ISSN1785 0037 (Online)
DOI: http://dx.doi.org/10.15666/aeer/2305_85678605

species, further confirming a diverse community (*Table 1*). The Pielou's Evenness Index value of 0.7742 indicates that individuals are relatively evenly distributed among species, while the Margalef's Richness Index value of 8.172 highlights high species richness (*Table 1*). These indices collectively demonstrate that the urban forest supports a balanced and diverse ecosystem, with no single species monopolizing resources.

Table 1. *Diversity indices of the entire urban forest in study area*

Diversity Index	Value
Shannon-Wiener Index	3.231
Simpson's Diversity Index (D)	0.056
Simpson's Index of Diversity (1 – D)	0.943
Pielou's Evenness Index	0.7742
Margalef's Richness Index (R)	8.172

At the plot level, species diversity exhibited considerable variability. The Berger-Parker Index, which measures the dominance of the most abundant species, had a median value of 0.6125, indicating moderate dominance by a few species (*Fig. 3*). The Margalef's Index, reflecting species richness, showed a median value of 0.692, with some plots being species-poor and others remarkably species-rich (*Fig. 3*). The Shannon-Wiener Index at the plot level had a median value of 0.690, suggesting moderate diversity (*Fig. 3*). However, the wide interquartile ranges (IQR) for these indices reveal significant variability across plots, with some areas exhibiting low diversity and others showing high diversity. For instance, the Shannon-Wiener Index ranged from 0 to 2.664, highlighting the spatial heterogeneity in species distribution (*Fig. 3*).

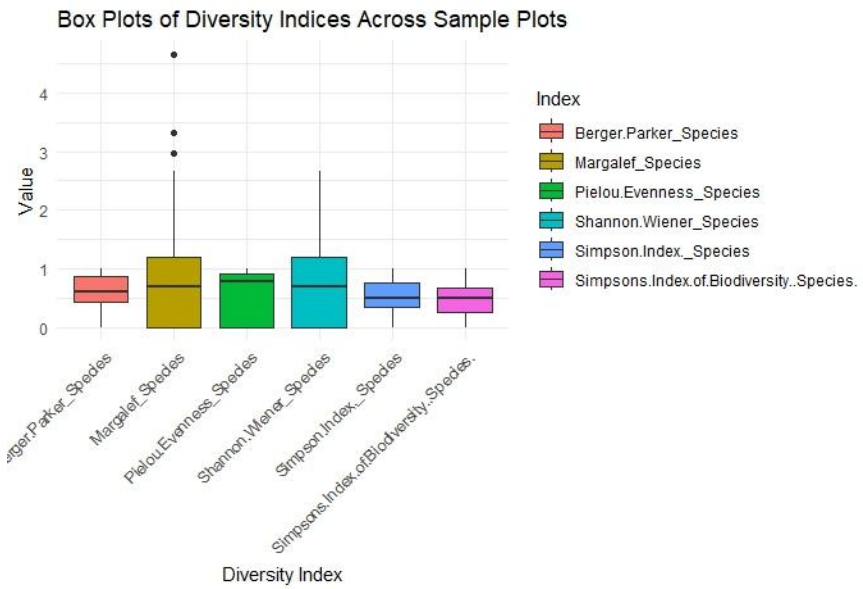

Figure 3. *Distribution of Diversity Indices Across Sample Plots*

The Importance Value Index (IVI) was used to identify ecologically dominant species. Populus tomentosa (IVI = 45.19), Sophora japonica (IVI = 37.31), and Salix matsudana (IVI = 19.94) emerged as the most dominant species, contributing significantly to the

http://www.aloki.hu ● ISSN 1589 1623 (Print) ● ISSN1785 0037 (Online)
DOI: http://dx.doi.org/10.15666/aeer/2305_85678605

forest structure (*Fig. 4*). These species exhibited high relative density, frequency, and dominance, underscoring their ecological importance. Other species, such as Ginkgo biloba, Juniperus chinensis, and Platanus orientalis, also played notable roles, with IVI values exceeding 10%. In contrast, 29 species had IVI values below 1, indicating their limited ecological impact despite contributing to overall biodiversity (*Fig. 5*).

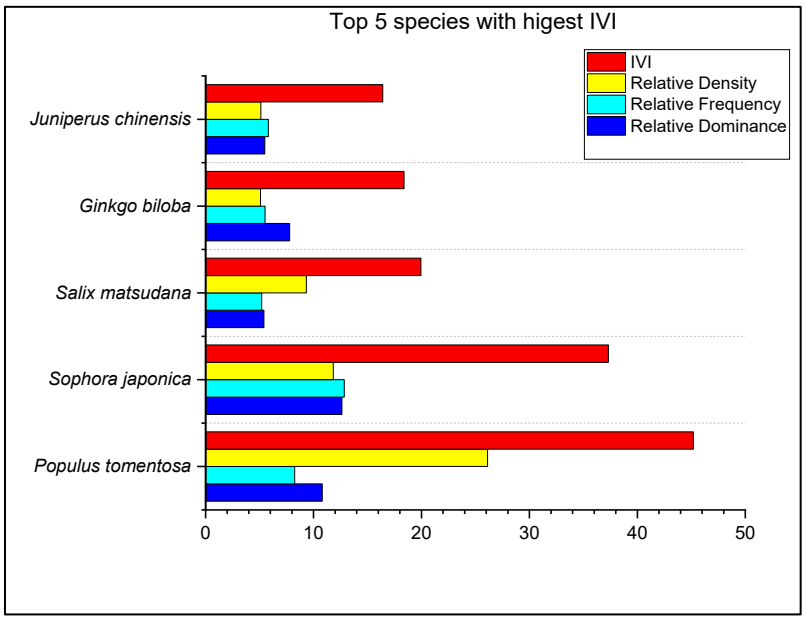

Figure 4. *Species with the highest IVI in the study area*

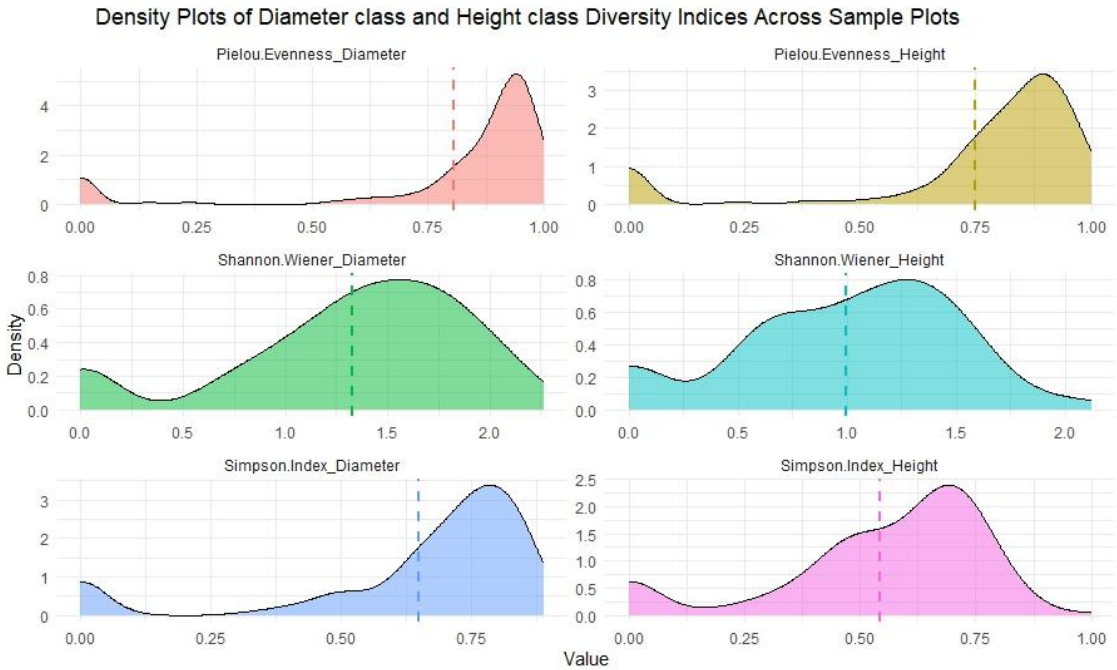

Figure 5. *Density plot of diameter and height class diversities across sample plots*

http://www.aloki.hu ● ISSN 1589 1623 (Print) ● ISSN1785 0037 (Online)
DOI: http://dx.doi.org/10.15666/aeer/2305_85678605

Structural complexity was further assessed through diameter and height class diversity. Diameter classes were divided into 21 intervals (4 cm each), and diversity indices were calculated. The Shannon-Wiener Index for diameter classes was 2.32, indicating moderate to high heterogeneity, while the Pielou's Evenness Index value of 0.74 suggested a relatively even distribution of diameter classes (*Table 2*). The Simpson Index value of 0.88 confirmed low dominance by any single diameter class. Similarly, height classes were divided into 14 intervals (2 m each), with the Shannon-Wiener Index for height classes being 2.09, reflecting moderate heterogeneity (*Fig. 5*). The Pielou's Evenness Index value of 0.77 and the Simpson Index value of 0.85 indicated a balanced distribution of height classes (*Table 2*). These findings suggest that the urban forest exhibits a structurally diverse canopy, with no single diameter or height class dominating the ecosystem. The combined analysis of height and diameter class diversity revealed moderate to high levels of heterogeneity and evenness across plots. The Pielou's Evenness Index for diameter and height classes was 0.917 and 0.843, respectively, indicating a relatively even distribution of both diameter and height classes. This balanced structure contributes to the overall resilience and ecological functionality of the urban forest.

Table 2. *Diversity indices of diameter class in study area*

Shannon-Winer index	Pielou's Evenness Index	Simpson Index
Diameter heterogenicity (*DH*)	Diameter distribution evenness and numbers of each diameter class (*DD*)	Evenness of diameter distribution (*DE*)
2.32	0.74	0.88

Stand structure

Canopy density

The average canopy density across all sampling plots, measured using a densiometer, was 46.87% (*Fig. 6*). Notably, eight plots exhibited 0% canopy cover. The distribution of canopy cover classes revealed that the highest number of sample plots (26) fell within the 31%-40% canopy cover class, followed by 19 plots in the 61%-70% class. Additionally, 18 plots each were recorded in the 11%-20%, 21%-30%, 41%-50%, and 71%-80% canopy cover classes. Overall, 97 sample plots had less than 50% crown cover, while 57 plots had crown cover exceeding 50% (*Fig. 6*).

Vegetation type

The urban forest is predominantly composed of broadleaf deciduous species, with a variety of stand types reflecting differing levels of species diversity and structural complexity. These stand types offer valuable insights into the biodiversity and ecological resilience of the urban forest ecosystem. The most prevalent stand type is the Broadleaf Mixed Forest, represented by 76 stands, which exhibits high species diversity within the broadleaf category (*Fig. 7*). This stand type is characterized by a mixture of deciduous tree species, likely forming a complex multi-layered structure with varying canopy densities. In contrast, the Broadleaf Pure Forest, comprising 26 stands, is dominated by a few broadleaf deciduous species. Although labeled "pure," this forest type likely includes secondary species such as *Ginkgo biloba*, *Populus tomentosa*, *Salix babylonica*, *Populus alba*, *Ailanthus altissima*, *Sophora japonica*, *Eucommia ulmoides*, and *Salix matsudana*.

http://www.aloki.hu ● ISSN 1589 1623 (Print) ● ISSN1785 0037 (Online)
DOI: http://dx.doi.org/10.15666/aeer/2305_85678605

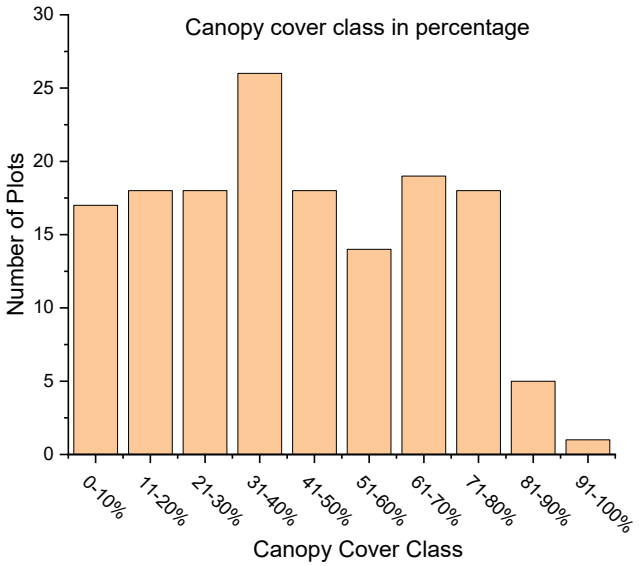

Figure 6. *Percentage of canopy cover in number of plots in study area*

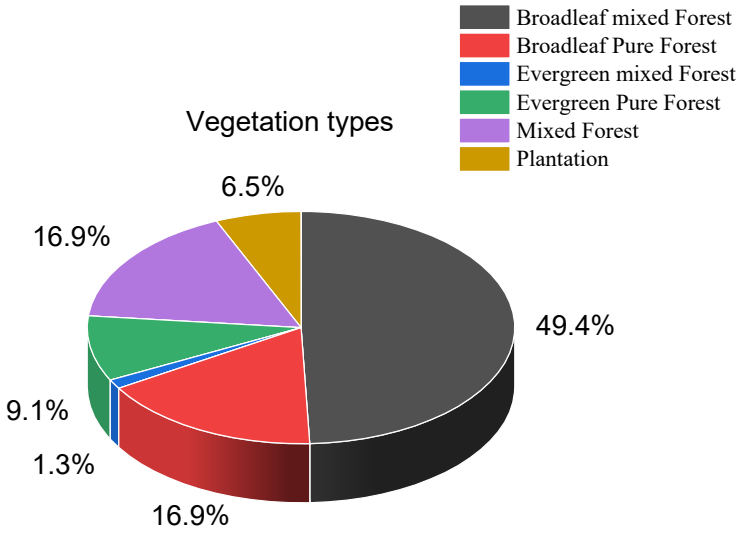

Figure 7. *Stand types of the urban forest*

Evergreen Mixed Forest, represented by only 2 stands, constitutes a very small proportion of the urban forest and is characterized by a mixture of evergreen coniferous and/or broadleaf species. Similarly, the Evergreen Pure Forest, with 14 stands, is predominantly composed of evergreen species, primarily dominated by *Pinus tabuliformis*, *Shorea negrosensis*, and *Juniperus chinensis* within each plot. Lastly, the Mixed Forest category, encompassing 26 stands, includes a combination of both deciduous and evergreen tree species, with no single species dominating (*Fig. 7*). This category also includes newly planted plots, reflecting ongoing efforts to enhance the forest's diversity and structure. Together, these stand types highlight the varied composition and structural complexity of the urban forest, contributing to its overall ecological functionality and resilience.

http://www.aloki.hu ● ISSN 1589 1623 (Print) ● ISSN1785 0037 (Online)
DOI: http://dx.doi.org/10.15666/aeer/2305_85678605

Stand density and growing stock

The stand density and growing stock of the urban forest were analyzed to assess tree distribution and biomass across the study area. The average stand density across all plots was 181.60 trees per hectare (trees/ha), with the highest density recorded at 855.56 trees/ha (*Fig. 8*). The interquartile range (IQR) of stand density spanned from approximately 100 to 300 trees/ha, indicating that the middle 50% of the data fell within this range. The median stand density was approximately 200 trees/ha, suggesting a moderate and healthy tree density in most plots. The IQR also demonstrated moderate variability in stand density among the plots, with most plots ranging between 100 and 300 trees/ha, reflecting a fairly consistent distribution of tree density across the urban forest (*Fig. 8*).

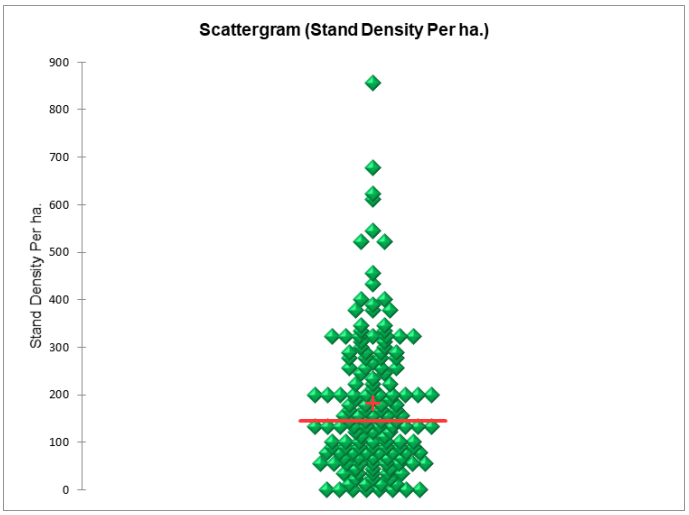

Figure 8. *Average stand density per hectare across the plots*

Species-wise stand density analysis revealed that out of the 65 recorded species, 41 had a stand density of less than 1 tree/ha (*Fig. 8*). The least dense species, including *Salix babylonica*, *Phoenix dactylifera*, *Pinus parviflora*, *Populus adenopoda*, *Malus domestica*, *Syzygium aromaticum*, *Picea wilsonii*, *Malus pumila*, *Tamarix chinensis*, *Hibiscus syriacus*, and *Hibiscus rosa-sinensis*, each had a stand density of 0.07 trees/ha (*Fig. 8*). In contrast, the top 10 species with the highest stand density were *Sophora japonica* (22.94 trees/ha), *Populus tomentosa* (19.62 trees/ha), *Ginkgo biloba* (14.14 trees/ha), *Pinus tabuliformis* (11.18 trees/ha), *Ligustrum lucidum* (10.68 trees/ha), *Juniperus chinensis* (9.96 trees/ha), *Platanus orientalis* (9.16 trees/ha), *Salix matsudana* (7.29 trees/ha), *Ailanthus altissima* (7.07 trees/ha), and *Eucommia ulmoides* (5.70 trees/ha) (*Fig. 8*). These species collectively represent the dominant components of the urban forest's tree density.

The growing stock of the forest was evaluated through plot-wise and species-wise basal area measurements (*Fig. 9*). The average basal area across the sample plots was 7,305.78 m²/ha, with the highest basal area recorded at 39,170.25 m²/ha (*Fig. 9*). Of the sample plots, 89 had basal areas below the average, while the remaining plots exceeded this value. Specifically, 42 plots had basal areas greater than 10,000 m²/ha, and 15 plots had basal areas less than 1,000 m²/ha (*Fig. 9*).

http://www.aloki.hu ● ISSN 1589 1623 (Print) ● ISSN1785 0037 (Online)
DOI: http://dx.doi.org/10.15666/aeer/2305_85678605

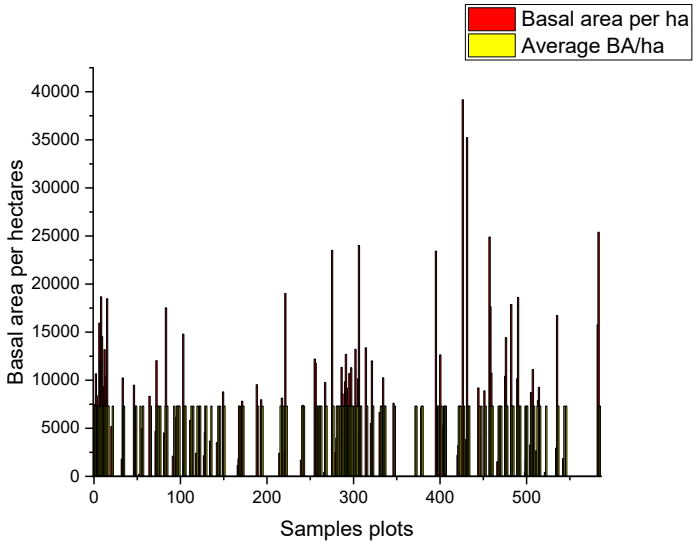

Figure 9. *Basal area of sample plots*

Species-wise, the top five species with the highest basal area per hectare were *Populus tomentosa* (293,935.41m²/ha), *Sophora japonica* (133,160.74 m²/ha), *Salix matsudana* (105,078.02 m²/ha), *Juniperus chinensis* (57,602.62 m²/ha), and *Platanus orientalis* (57,581.74 m²/ha) (*Fig. 10*). Notably, seven species namely *Populus tomentosa*, *Sophora japonica*, *Salix matsudana*, *Juniperus chinensis*, *Platanus orientalis*, *Ginkgo biloba*, and *Ligustrum lucidum* accounted for approximately 67% of the total basal area, underscoring their significant contribution to the forest's biomass and structural complexity (*Fig. 10*). These findings highlight the variability in stand density and growing stock across the urban forest, reflecting both the diversity and dominance of key species within the ecosystem.

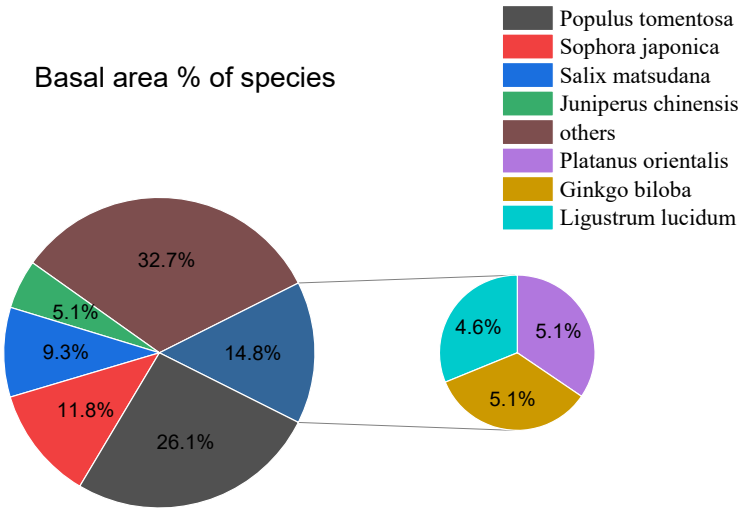

Figure 10. *Basal area proportion of different species*

http://www.aloki.hu ● ISSN 1589 1623 (Print) ● ISSN1785 0037 (Online)
DOI: http://dx.doi.org/10.15666/aeer/2305_85678605

Biomass calculation

Urban trees provide a range of critical ecological services, and accurate estimation of tree biomass is essential for sustainable urban development. This section presents the analysis of aboveground biomass (AGB), belowground biomass (BGB), and total biomass across the urban forest, along with their distribution by species, diameter class, and height class (*Table 3*). The highest aboveground biomass recorded in a single plot was 23,739.05 kg, with an average of 3,279.08 kg per plot, translating to an average of 36,434.33 kg/ha across all plots (*Fig. 11*). Belowground biomass peaked at 4,713.41 kg in one plot, with an average of 619.03 kg per plot, resulting in an average of 6,878.11 kg/ha (*Fig. 11*). The total biomass, combining both aboveground and belowground components, reached a maximum of 26,184.02 kg in a single plot, with an average of 3,898.11 kg per plot, yielding an average total biomass of 43,312.33 kg/ha (*Fig. 11*). The distribution of biomass across plots showed significant variability, with a wide interquartile range (IQR) for AGB (3,423.78 kg), BGB (568.50 kg), and total biomass (4,009.70 kg). The median values for AGB (2,092.00 kg), BGB (508.55 kg), and total biomass (2,557.84 kg) indicated that half of the plots had biomass values above these thresholds, while the other half fell below. The large range between the lower and upper whiskers for AGB (9.73–9,425.01 kg), BGB (0.90–1,626.91 kg), and total biomass (10.63–11,178.47 kg) highlighted substantial variability, with some plots exhibiting extremely low biomass and others exceptionally high (*Fig 10*).

Table 3. *Statistics of biomass distribution across plots*

Metric	Mean	Median	Q1	Q3	IQR	Lower Whisker	Upper Whisker
Aboveground (AGB)	3279.08	2092.00	865.55	4289.33	3423.78	9.73	9425.01
Belowground Biomass (BGB)	619.03	508.55	205.67	774.17	568.50	0.90	1626.91
Total Biomass (AGB+BGB)	3898.11	2557.84	1154.21	5163.91	4009.70	10.63	11178.47

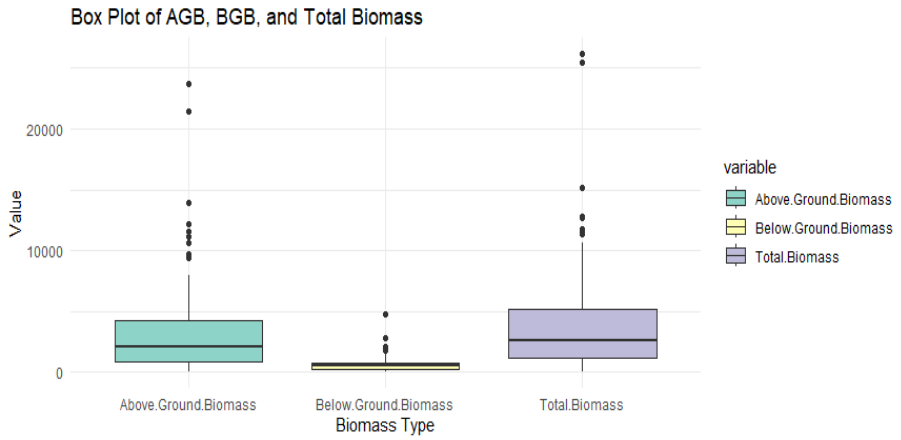

Figure 11. *Plot-Wise biomass distribution in study area*

Species-wise analysis revealed that *Populus tomentosa* contributed the most to total biomass, accounting for 26.81%, followed by *Sophora japonica* (12.86%), *Ginkgo* contributed *biloba* (10.27%), and *Salix matsudana* (9.59%) (*Fig. 12*). In contrast, 49

http://www.aloki.hu ● ISSN 1589 1623 (Print) ● ISSN1785 0037 (Online)
DOI: http://dx.doi.org/10.15666/aeer/2305_85678605

species each less than 1% to the total biomass, underscoring the dominance of a few key species in the urban forest's biomass structure.

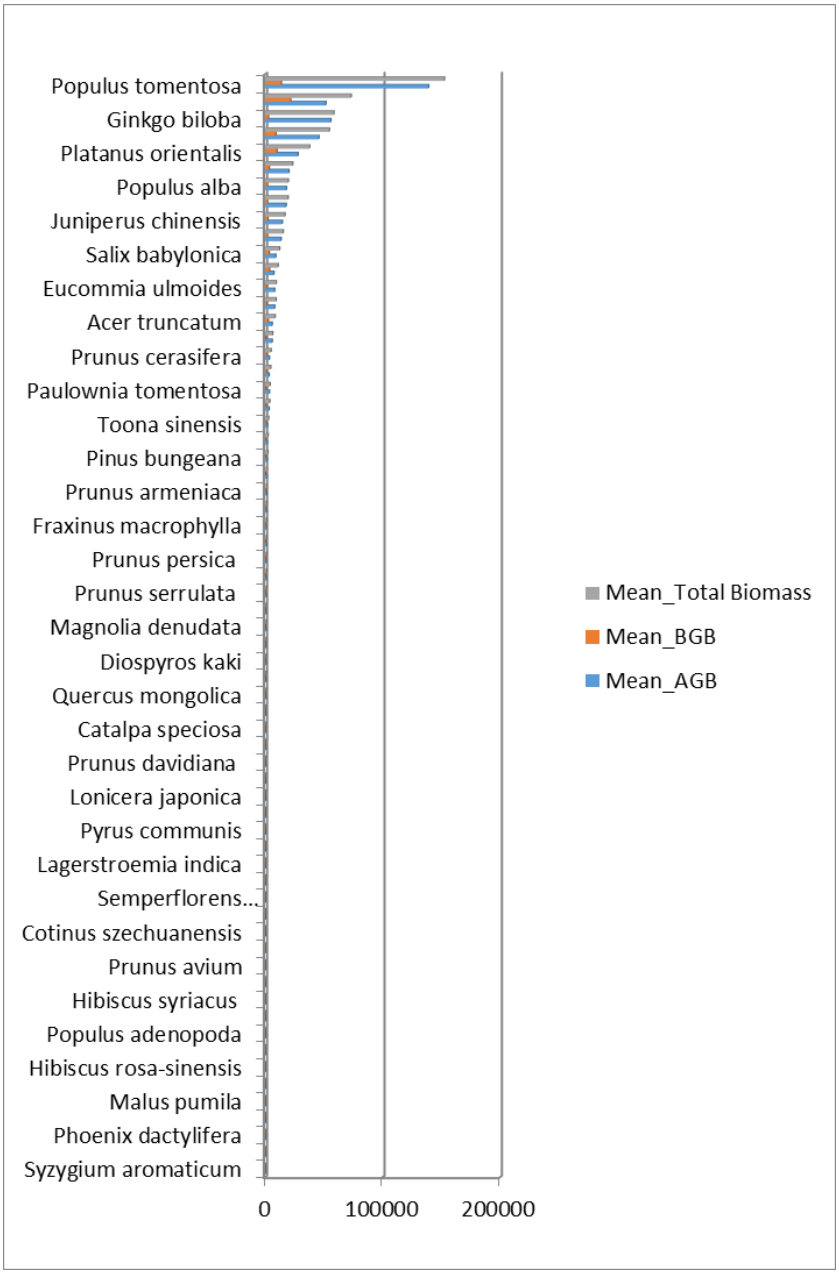

Figure 12. *Species-Wise biomass contribution*

The distribution of biomass across diameter classes provided insights into the structural composition and productivity of the urban forest. Aboveground biomass peaked in the 32–35.9 cm diameter class (53,146.88 kg), followed by the 28–31.9 cm (52,700.17 kg) and 24–27.9 cm (52,113.23 kg) classes (*Fig. 11*). Belowground biomass followed a similar trend, with the highest values in the 32–35.9 cm class (11,387.05 kg) (*Fig. 11*). Total biomass also peaked in the 32–35.9 cm class (64,533.94 kg), indicating that medium-sized trees (24–35.9 cm) contributed the most to biomass accumulation.

http://www.aloki.hu ● ISSN 1589 1623 (Print) ● ISSN1785 0037 (Online)
DOI: http://dx.doi.org/10.15666/aeer/2305_85678605

Smaller diameter classes (4–15.9 cm) contributed only 6% to the total biomass, reflecting limited contributions from young trees (*Fig 13*). The decrease in biomass in larger diameter classes (40 cm and above) suggested a lower density of large trees in the urban forest (*Fig 13*).

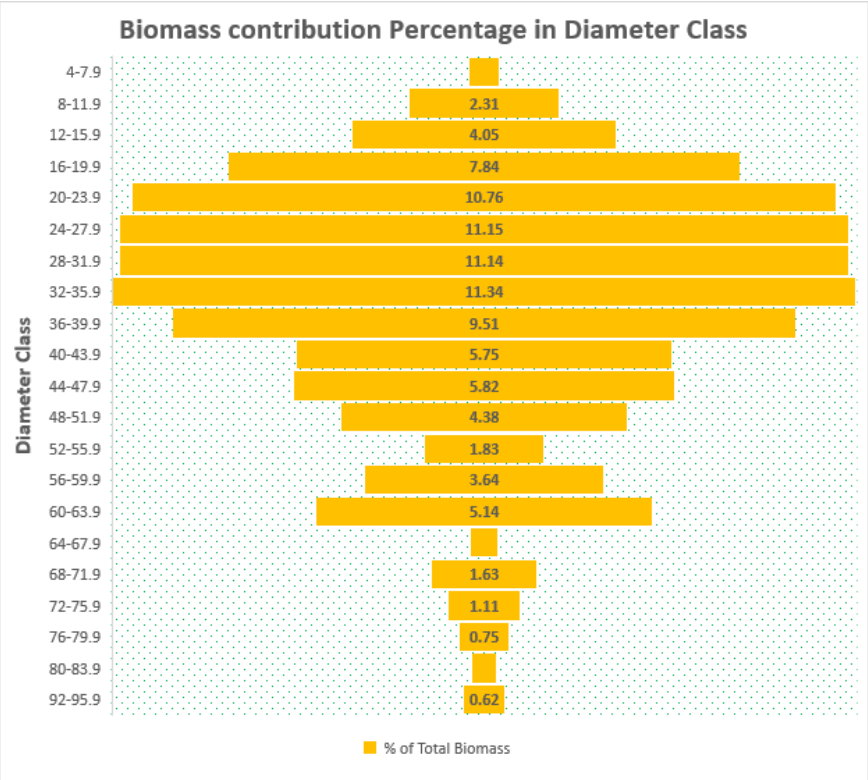

Figure 13. *Biomass distribution ccross diameter classes*

Height class analysis revealed that aboveground biomass peaked in the 8–9.9 m class (94,989.11 kg), followed by the 10–11.9 m (88,569.17 kg) and 6–7.9 m (48,742.17 kg) classes. Belowground biomass also peaked in the 8–9.9 m class (19,250.82 kg), with similar trends observed in adjacent height classes. Total biomass reached its maximum in the 8–9.9 m class (114,239.93 kg), indicating that trees within this height range contributed the most to overall biomass. The 8–9.9 m class alone accounted for 20.07% of the total biomass, while smaller height classes (0–5.9 m) contributed only 4.43% (*Fig. 14*). The gradual decline in biomass contributions from taller height classes (12 m and above) suggested a lower density of very tall trees.

The biomass distribution analysis revealed a unimodal pattern, with medium-sized trees (24–35.9 cm diameter) and medium-height trees (8–11.9 m) contributing the most to total biomass. This indicates a relatively mature stand with a significant proportion of trees in their optimal growth stages. The dominance of a few species, such as *Populus tomentosa* and *Sophora japonica*, in biomass contribution highlights their ecological importance in the urban forest. The limited contributions from smaller diameter and height classes suggest a lower density of young trees, while the decline in biomass in larger diameter and height classes reflects fewer mature trees. Overall, the biomass distribution underscores the structural complexity and productivity of the urban forest, providing valuable insights for its management and conservation.

http://www.aloki.hu ● ISSN 1589 1623 (Print) ● ISSN1785 0037 (Online)
DOI: http://dx.doi.org/10.15666/aeer/2305_85678605

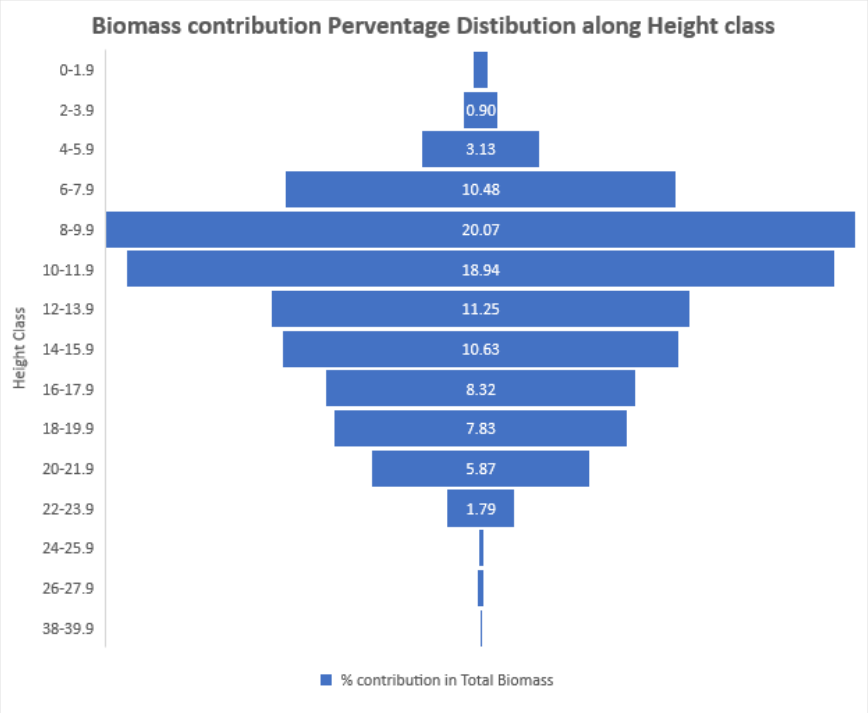

Figure 14. *Biomass distribution in relation to height class*

Carbon stock calculation

The carbon stock of the urban forest was calculated by assessing biomass carbon and soil carbon across the sampling plots, providing insights into the carbon sequestration potential and variability within the ecosystem. The average biomass carbon stock across the plots was 1,736.94 kg, with values ranging from 0 kg to 12,306.48 kg, indicating significant variability (*Fig. 15*). The high maximum value suggests the presence of outliers or plots with exceptionally high biomass carbon. The standard deviation (SD = 1,911.64) relative to the mean highlight's considerable variability in biomass carbon across the plots. The positive skewness (2.54) indicates that most plots have lower biomass carbon values, with a few plots exhibiting very high values that skew the distribution (*Table 4*). The high kurtosis value (9.78) further confirms a distribution with heavy tails, reflecting the presence of outliers (*Table 4*). Biomass density averaged 19,299.32 kg/ha, with a range of 0–136,738.75 kg/ha, underscoring the substantial variability in biomass accumulation across the plots (*Fig. 15*). The high standard deviation (21,240.40) and skewness (2.54) suggest that while most plots have moderate biomass densities, a few plots contribute disproportionately to the overall carbon stock (*Table 4*).

Soil carbon stock exhibited less variability compared to biomass carbon, with a mean of 509.96 kg and a median of 471.15 kg, indicating a more symmetrical distribution (*Fig. 15*). The standard deviation (189.51) was relatively low, reflecting moderate variability across the plots. Soil carbon density averaged 5,666.17 kg/ha, with a range of 1,911.60–15,882.00 kg/ha (*Fig. 15*). The close values of the mean and median, along with the lower standard deviation (2,105.68), suggest a more consistent distribution of soil carbon compared to biomass carbon. However, the positive skewness (1.71) and kurtosis

http://www.aloki.hu ● ISSN 1589 1623 (Print) ● ISSN1785 0037 (Online)
DOI: http://dx.doi.org/10.15666/aeer/2305_85678605

(4.79) indicate that some plots still have higher soil carbon values, contributing to a slightly skewed distribution (*Table 4*).

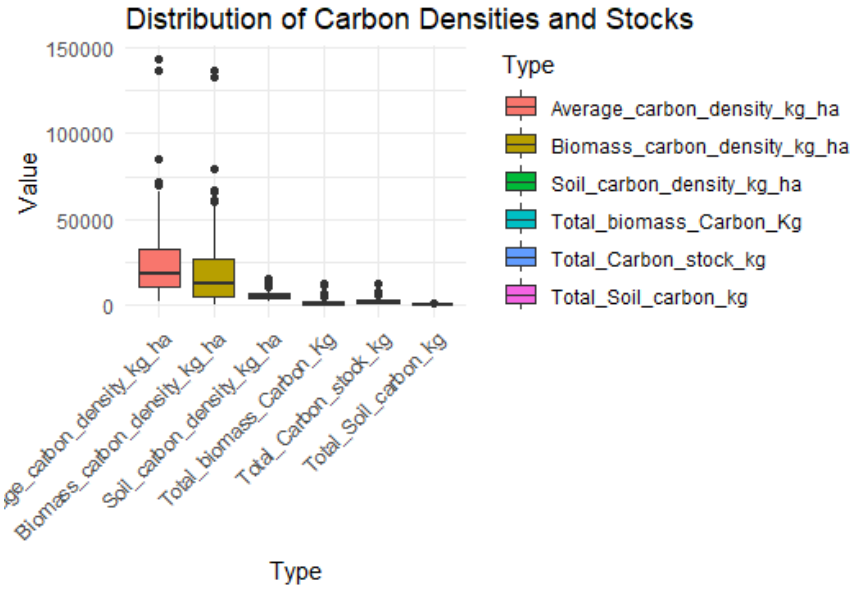

Figure 15. *Distribution of carbon density and carbon stock across sample plots*

Table 4. *Statistics of carbon density and carbon stock distribution across sample plots*

Biomass/Carbon	Mean	Median	Minimum Biomass	Maximum Biomass	SD	SE	Skewness	Kurtosis
Biomass Carbon (Kg)	1736.94	1131.26	0	12306.48	1911.64	154.04	2.54	9.78
Biomass Density (kg/ha)	19299.32	12569.65	0	136738.75	21240.40	1711.60	2.54	9.78
Soil Carbon (Kg)	509.96	471.15	172.04	1429.38	189.51	15.27	1.71	4.79
Soil Carbon Density (Kg/ha)	5666.17	5235	1911.6	15882	2105.68	169.68	1.71	4.79
Total Carbon Stock (Kg)	2284.69	1692.11	232.90	12920.03	1945.29	156.76	2.42	9.04
Average Carbon Density Kg/ha	25385.46	18801.31	2587.80	143555.95	21614.28	1741.73	2.42	9.04

The total carbon stock, combining biomass and soil carbon, ranged from 232.90 kg to 12,920.03 kg, with an average of 2,284.69 kg per plot. The high standard deviation (1,945.29) and significant disparity between the mean and median (1,692.11 kg) indicate a skewed distribution, driven by plots with exceptionally high carbon values. Average carbon density across the plots was 25,385.46 kg/ha, with a range of 2,587.80–143,555.95 kg/ha. The wide range and high standard deviation (21,614.28) reflect extreme variability, further emphasizing the influence of a few plots with very high carbon densities. The positive skewness (2.42) and kurtosis (9.04) confirm the presence of outliers and a heavy-tailed distribution (*Table 4*).

http://www.aloki.hu ● ISSN 1589 1623 (Print) ● ISSN1785 0037 (Online)
DOI: http://dx.doi.org/10.15666/aeer/2305_85678605

The analysis of carbon stock distribution reveals significant variability in both biomass and soil carbon across the urban forest. Biomass carbon exhibits higher variability and skewness, driven by a few plots with exceptionally high values, while soil carbon shows a more symmetrical distribution with moderate variability. The total carbon stock is heavily influenced by biomass carbon, with a few plots contributing disproportionately to the overall carbon sequestration potential. These findings highlight the importance of targeted management strategies to enhance carbon storage in areas with lower carbon densities while maintaining the high carbon stocks in outlier plots. The results underscore the urban forest's role in carbon sequestration and provide a foundation for future efforts to optimize its ecological benefits (Li, 2023).

Correlation between structural characteristics and total biomass

The relationship between structural characteristics (diameter class and height class) and total biomass was analyzed using Pearson correlation and linear regression methods. These analyses aimed to quantify the strength and direction of the relationships and to determine how changes in diameter and height classes influence total biomass.

The Pearson correlation coefficient between diameter class and total biomass was -0.592, indicating a moderate negative linear relationship. This suggests that, on average, as the diameter class increases, total biomass tends to decrease. The standard deviation of the diameter midpoint (27.13 cm) and total biomass (23,215.02 kg) highlights significant variability in both variables, implying that factors other than diameter may also influence biomass (*Fig. 16*). Linear regression analysis further supported this relationship, with a regression coefficient of -0.00069207, indicating a slight decrease in total biomass as diameter class increases. The t-value of -3.36799690 and a p-value of 0.002908385 (significant at $p < 0.05$) confirmed that this negative relationship is statistically significant (*Fig. 15*). This suggests that larger diameter classes, which typically represent older or larger trees, are associated with lower total biomass, possibly due to fewer trees in these classes.

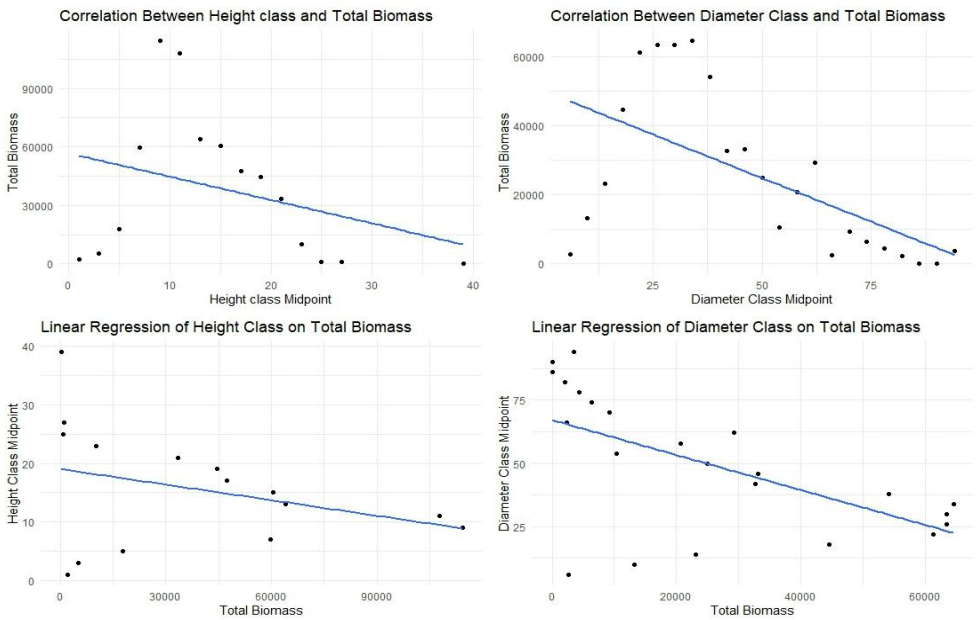

Figure 16. *Linear regression and correlation of total biomass with diameter class and height class*

http://www.aloki.hu ● ISSN 1589 1623 (Print) ● ISSN1785 0037 (Online)
DOI: http://dx.doi.org/10.15666/aeer/2305_85678605

The correlation coefficient between height class and total biomass was -0.326, indicating a weak negative relationship (*Fig. 16*). This implies that, on average, as the height class increases, total biomass tends to decrease slightly. The standard deviation for height class (10.33) and total biomass (37,975.95 kg) further emphasizes the variability in biomass values, even within the same height class. Linear regression analysis revealed a very weak negative relationship, with a regression coefficient of -0.00008863 (*Table 5*). However, the t-value of -1.24293786 and a p-value of 0.23584218 (greater than 0.05) indicated that this relationship is not statistically significant (*Table 5*). This suggests that height class alone is not a strong predictor of total biomass, and other factors likely play a more significant role in determining biomass accumulation.

Table 5. *Linear regression analysis of tree diameter class & tree height class on total biomass*

Diameter Class on Biomass	(Intercept)	67.12490719	6.90069159	9.72727246	3.14E-09
	Total biomass	-0.00069207	0.00020548	-3.36799690	0.002908385*
Height Class on Biomass	(Intercept)	19.02958225	3.76365236	5.05614771	0.000220056
	Total biomass	-0.00008863	0.00007131	-1.24293786	0.23584218

*Significant at 0.05

The analysis revealed a moderate negative correlation between diameter class and total biomass, with larger diameter classes associated with lower biomass. This relationship was statistically significant, indicating that diameter class is a meaningful predictor of biomass. In contrast, the relationship between height class and total biomass was weak and not statistically significant, suggesting that height class alone does not strongly influence biomass. The high variability in both diameter and height classes, as well as in total biomass, underscores the complexity of biomass accumulation in the urban forest. These findings highlight the importance of considering multiple structural and environmental factors when assessing biomass distribution and carbon sequestration potential in urban forests. Future studies could explore additional variables, such as species composition, stand density, and environmental conditions, to better understand the drivers of biomass variability.

Impact of stand attributes on carbon density

Normality checks are a critical step in statistical analysis, as many parametric tests, such as t-tests and ANOVA, assume that the data follows a normal distribution. Deviations from normality can lead to inaccurate results, making it essential to verify the distribution of the data before selecting appropriate statistical methods. The Shapiro-Wilk test was employed to assess the normality of biomass carbon density, soil carbon density, and total carbon density (*Table 6*). This test is particularly reliable for small to medium-sized samples, as it calculates a W statistic to determine deviations from a normal distribution, with lower W values indicating greater deviations.

The results of the Shapiro-Wilk test revealed that the data for biomass carbon density, soil carbon density, and total carbon density are not normally distributed. The W values for biomass carbon density (0.763937), soil carbon density (0.876097), and total carbon density (0.784592) were all associated with p-values far below the conventional significance threshold of 0.05 (*Fig. 17*). These low p-values led to the rejection of the null

http://www.aloki.hu ● ISSN 1589 1623 (Print) ● ISSN1785 0037 (Online)
DOI: http://dx.doi.org/10.15666/aeer/2305_85678605

hypothesis, which assumes that the data is normally distributed. Consequently, non-parametric tests, such as the Kruskal-Wallis test and Spearman's Rank Correlation, were deemed appropriate for analyzing the relationships between species diversity, stand structure, and carbon density. These tests do not rely on the assumption of normality, making them suitable for datasets with non-normal distributions.

Table 6. *Shapiro-Wilk normality test for biomass carbon density, soil carbon density, and total carbon density*

Column	W. W	p_value	Normality
Biomass Carbon Density	0.763937	1.83E-14	Not Normal
Soil Carbon Density	0.876097	9.64E-10	Not Normal
Total Carbon Density	0.784592	1.99E-13	Not Normal

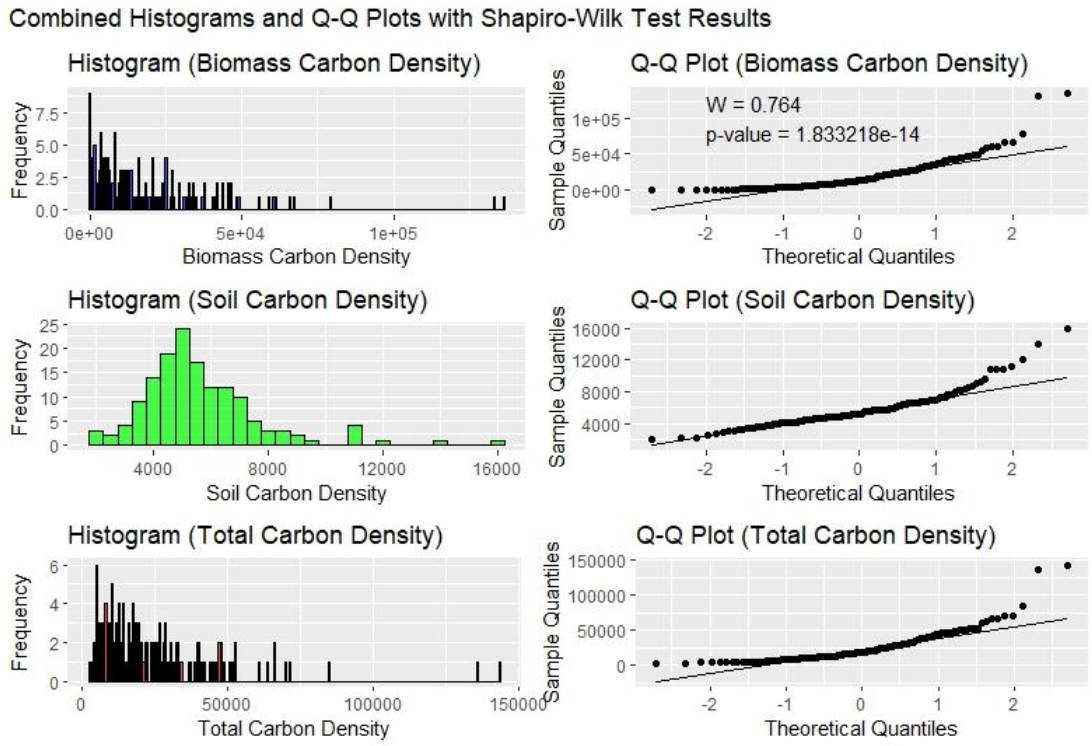

Figure 17. *Normality test using Shapiro-Wilk test*

The non-normal distribution of the data highlights the variability and complexity of carbon density measurements in the urban forest. This variability may be influenced by factors such as species composition, stand age, and environmental conditions, which can lead to skewed or non-normal distributions. By using non-parametric methods, the analysis can more accurately capture the relationships between stand attributes and carbon density, providing a robust foundation for understanding the factors driving carbon sequestration in the urban forest ecosystem.

http://www.aloki.hu ● ISSN 1589 1623 (Print) ● ISSN1785 0037 (Online)
DOI: http://dx.doi.org/10.15666/aeer/2305_85678605

Impact of stand attributes on carbon density

The Kruskal-Wallis test, a non-parametric method, was employed to assess statistically significant relationships between structural attributes (diversity indices and stand structure) and carbon density. This test is suitable for non-normally distributed data, as it evaluates differences in medians across three or more independent groups without assuming normality. Similarly, Spearman's rank correlation was used to measure the strength and direction of association between two ranked variables. This non-parametric method evaluates how well the relationship between variables can be described using a monotonic function, making it ideal for analyzing the non-normal distribution of species diversity, stand structure, and carbon density data. Together, these methods provide robust insights into the factors influencing carbon density in the urban forest.

Impact of stand diversity on biomass carbon density

Kruskal-Wallis test

The Kruskal-Wallis test was used to assess the impact of stand diversity on biomass carbon density, focusing on species, diameter, and height class diversity (*Fig. 18*). Results showed no significant differences in biomass carbon density across various levels of species diversity ($p > 0.05$ for Shannon-Wiener, Simpson's, and Pielou's indices) (*Fig. 18*).

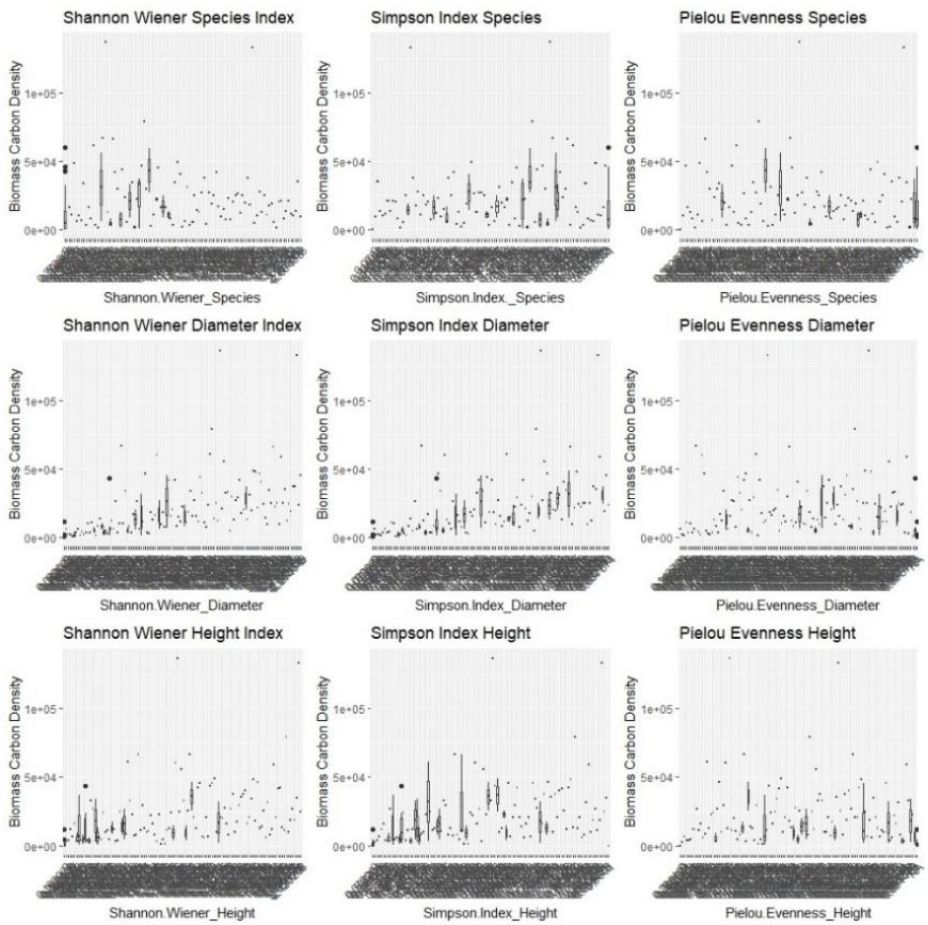

Figure 18. *Kruskal-Wallis test assessing the impact of stand diversity on biomass carbon density*

http://www.aloki.hu ● ISSN 1589 1623 (Print) ● ISSN1785 0037 (Online)
DOI: http://dx.doi.org/10.15666/aeer/2305_85678605

Similarly, diameter and height class diversity indices did not significantly influence biomass carbon density, except for Simpson's Diameter Index, which showed marginal significance ($p = 0.057$) (*Fig. 18*). These findings suggest that species, diameter, and height diversity have minimal impact on biomass carbon density, indicating that other factors, such as environmental conditions or land use practices, may play a more critical role.

Spearman correlation test

Spearman's correlation analysis revealed varying relationships between diversity indices and biomass carbon density. Species diversity showed a weak positive correlation with biomass carbon density (Shannon-Wiener Index: $r = 0.274$, $p = 0.0006$), while diameter class diversity exhibited strong positive correlations (Shannon-Wiener: $r = 0.746$, $p < 0.0001$; Simpson's: $r = 0.721$, $p < 0.0001$). Height class diversity also showed moderate positive correlations (Shannon-Wiener: $r = 0.593$, $p < 0.0001$; Simpson's: $r = 0.539$, $p < 0.0001$) (*Fig. 19*). These results highlight that structural diversity, particularly in diameter and height classes, has a stronger influence on biomass carbon density than species diversity.

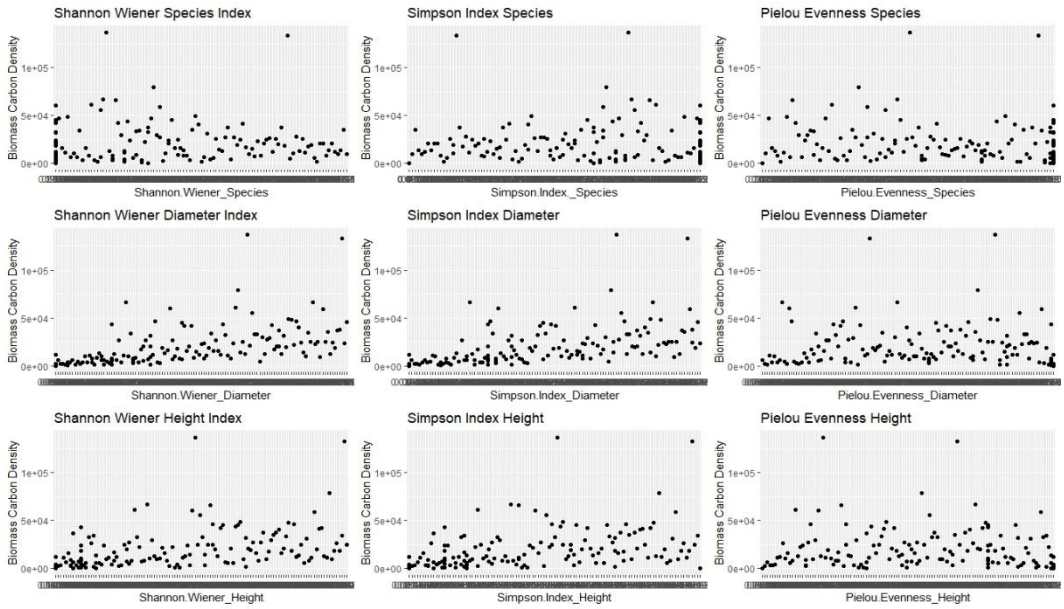

Figure 19. *Correlation between stand diversity and biomass carbon density*

Impact of stand structure on biomass carbon density

The Kruskal-Wallis test revealed significant relationships between specific stand structure parameters and biomass carbon density. Stand type ($p = 0.010$), canopy density ($p = 0.002$), and stand density ($p = 0.0003$) were found to significantly influence biomass carbon density (*Fig. 20*). This suggests that the type of forest stand (e.g., mixed forest, pure forest), the density of the canopy, and the number of trees per hectare play crucial roles in determining the amount of carbon stored in biomass. In contrast, average tree height, average diameter at breast height (DBH), and basal area did not show significant relationships with biomass carbon density ($p > 0.05$), indicating that these factors are less influential in this context (*Fig. 20*).

http://www.aloki.hu ● ISSN 1589 1623 (Print) ● ISSN1785 0037 (Online)
DOI: http://dx.doi.org/10.15666/aeer/2305_85678605

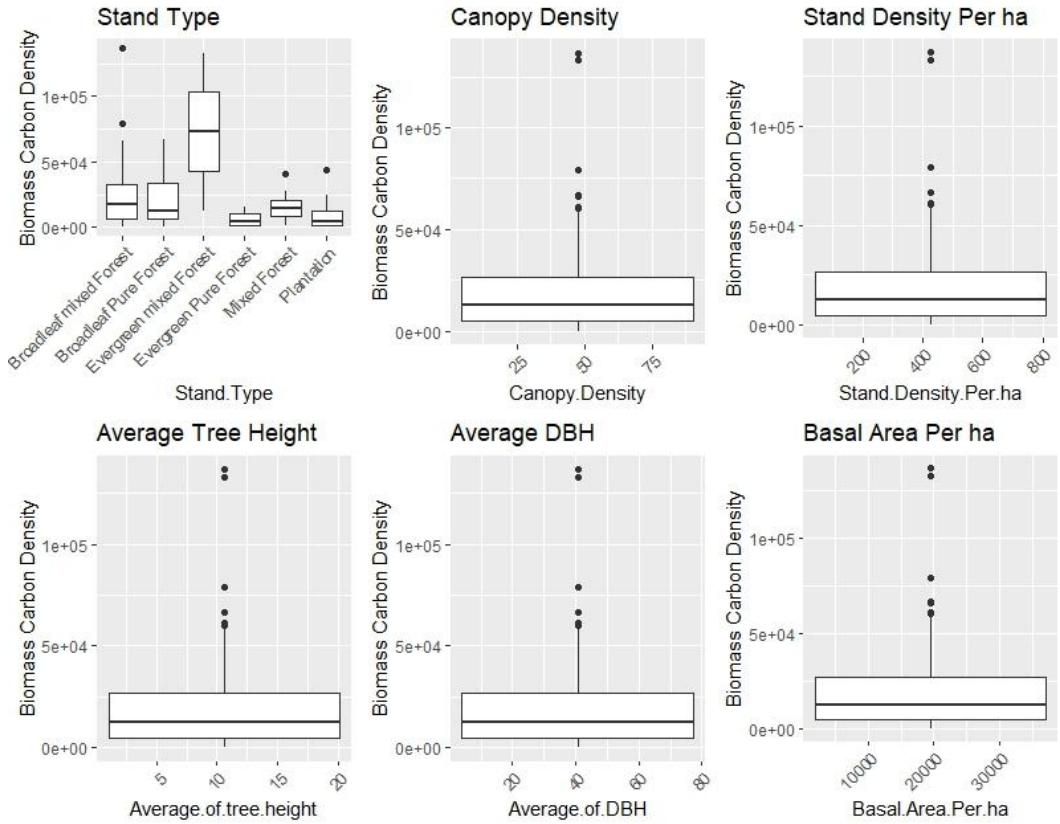

Figure 20. *Box plots for the Kruskal-Wallis test on the impact of stand structure on biomass carbon density*

Spearman's correlation analysis further supported these findings. Basal area exhibited the strongest positive correlation with biomass carbon density ($r = 0.923$, $p < 0.0001$), highlighting that stands with larger basal areas tend to store more carbon due to greater tree biomass. Stand density also showed a substantial positive correlation ($r = 0.488$, $p < 0.0001$), suggesting that higher tree densities contribute to increased carbon storage, likely due to more trees accumulating biomass (*Fig. 21*). Canopy density demonstrated a moderate positive correlation ($r = 0.306$, $p < 0.0001$), indicating that denser canopies, which capture more sunlight and promote higher photosynthetic activity, are associated with greater biomass carbon density (*Fig. 21*).

Interestingly, stand type showed a weak negative correlation ($r = -0.183$, $p = 0.023$), implying that certain stand types, such as pure forests or specific species compositions, may have lower biomass carbon densities compared to others (*Fig. 21*). This could be due to differences in growth rates, species-specific biomass accumulation, or ecological functions among stand types. Overall, these results underscore the importance of stand structure, particularly basal area, stand density, and canopy density, in influencing biomass carbon density. While species diversity and average tree metrics (height and DBH) are less impactful, structural attributes play a critical role in carbon sequestration. These findings provide valuable insights for urban forest management, emphasizing the need to prioritize structural diversity and composition to enhance carbon storage and promote sustainable urban ecosystems (Feng et al., 2024).

http://www.aloki.hu ● ISSN 1589 1623 (Print) ● ISSN1785 0037 (Online)
DOI: http://dx.doi.org/10.15666/aeer/2305_85678605

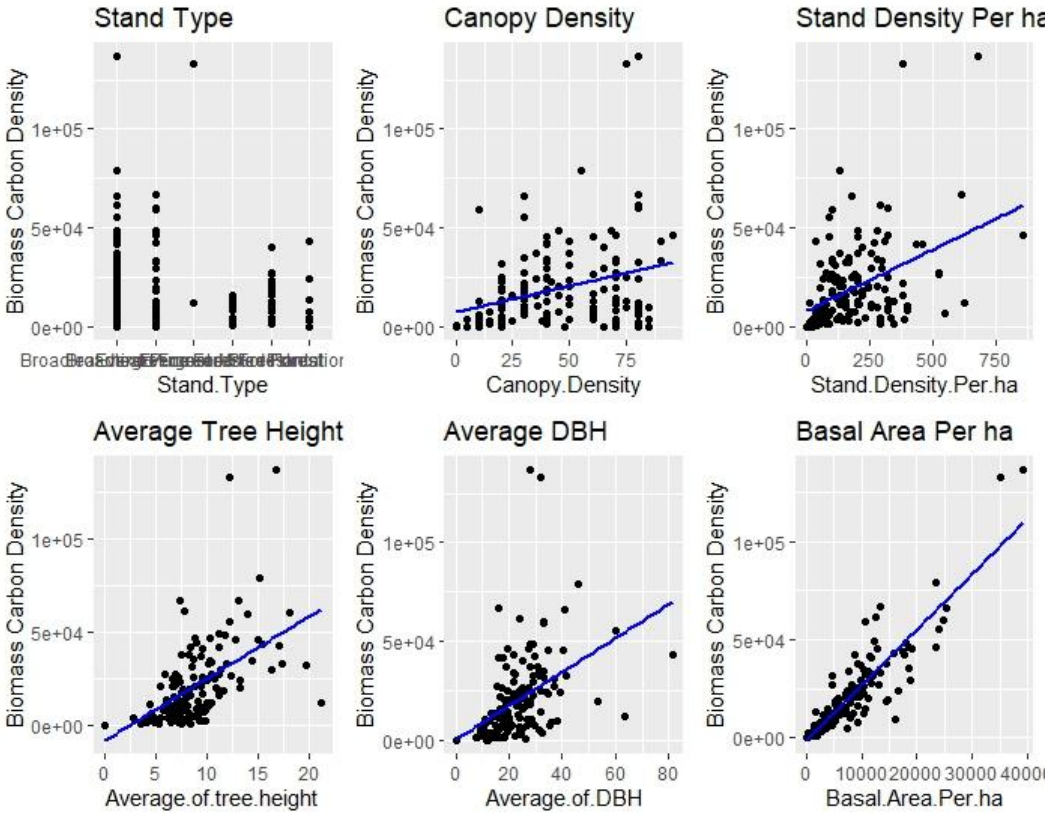

Figure 21. *Spearman correlation between stand structure and biomass carbon density*

The analysis indicates that structural attributes, such as diameter and height class diversity, basal area, and stand density, have a stronger influence on biomass carbon density than species diversity. These findings emphasize the importance of considering stand structure in urban forest management to enhance carbon sequestration. While species diversity plays a role, structural diversity and stand composition are more critical determinants of biomass carbon density.

Impact of stand diversity on soil carbon density

Kruskal-Wallis test

The Kruskal-Wallis test was conducted to assess the relationship between stand diversity indices and soil carbon density (*Fig. 22*). Results indicated no statistically significant relationships between any of the nine diversity indices including species diversity (Shannon-Wiener, Simpson's, and Pielou's indices), diameter class diversity, and height class diversity and soil carbon density. All p-values were well above the conventional significance threshold of 0.05, with the highest p-value being 0.547 for Simpson's Diameter Index (*Fig. 22*). This suggests that variations in species, diameter, and height diversity do not significantly explain differences in soil carbon density. The lack of significance across all indices implies that other factors, such as soil type, land use history, or environmental conditions, may play a more dominant role in influencing soil carbon density. Visual inspection of boxplots further supported these findings, showing relatively consistent distributions of soil carbon density across different diversity index values.

http://www.aloki.hu ● ISSN 1589 1623 (Print) ● ISSN1785 0037 (Online)
DOI: http://dx.doi.org/10.15666/aeer/2305_85678605

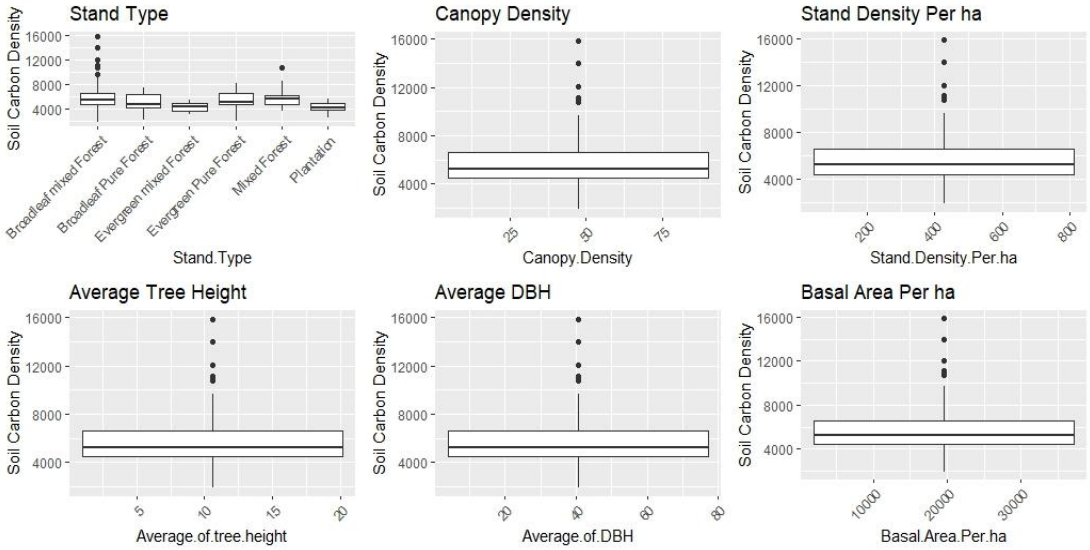

Figure 22. *Kruskal-Wallis test for the impact of stand structure on soil carbon density*

Spearman correlation test

Spearman's rank correlation analysis revealed weak to negligible relationships between most diversity indices and soil carbon density. Species diversity indices, such as Shannon-Wiener ($r = 0.09$, $p = 0.26$), Simpson's ($r = -0.06$, $p = 0.45$), and Pielou's Evenness ($r = 0.08$, $p = 0.38$), showed no significant correlations. Similarly, height class diversity indices, including Shannon-Wiener ($r = -0.07$, $p = 0.41$), Simpson's ($r = -0.05$, $p = 0.58$), and Pielou's Evenness ($r = 0.06$, $p = 0.48$), also exhibited non-significant relationships (*Fig. 23*). However, diameter class diversity indices showed slightly stronger, albeit weak, positive correlations. Pielou's Evenness Diameter demonstrated a statistically significant positive correlation ($r = 0.20$, $p = 0.02$), suggesting that greater evenness in diameter distribution is associated with slightly higher soil carbon density. Simpson's Diameter Index ($r = 0.16$, $p = 0.06$) and Shannon-Wiener Diameter ($r = 0.15$, $p = 0.07$) also showed weak positive trends, though these were only marginally significant (*Fig. 23*).

The analysis indicates that species and height class diversity have minimal impact on soil carbon density, while diameter class diversity shows a weak but notable influence. The significant but modest correlation between diameter evenness and soil carbon density suggests that the distribution of tree diameters within a stand may play a role in soil carbon accumulation, possibly due to differences in root systems, litterfall, or microclimate conditions. However, the overall lack of strong correlations highlights the complexity of soil carbon dynamics, which are likely influenced more by external factors such as soil properties, land management practices, and environmental conditions. These findings underscore the need for further research into the drivers of soil carbon density and suggest that stand diversity metrics alone may not be sufficient to predict soil carbon storage in urban forests.

Modeling carbon density with generalized additive models

The analysis aimed to identify ecological predictors of carbon density in forested ecosystems using GAMs. GAMs were chosen for their ability to capture non-linear

http://www.aloki.hu ● ISSN 1589 1623 (Print) ● ISSN1785 0037 (Online)
DOI: http://dx.doi.org/10.15666/aeer/2305_85678605

relationships between carbon density and predictor variables, such as species diversity, diameter class diversity, height class diversity, and stand characteristics. This approach provides a flexible framework to model complex ecological data, enabling evidence-based decisions for sustainable forest management and climate change mitigation.

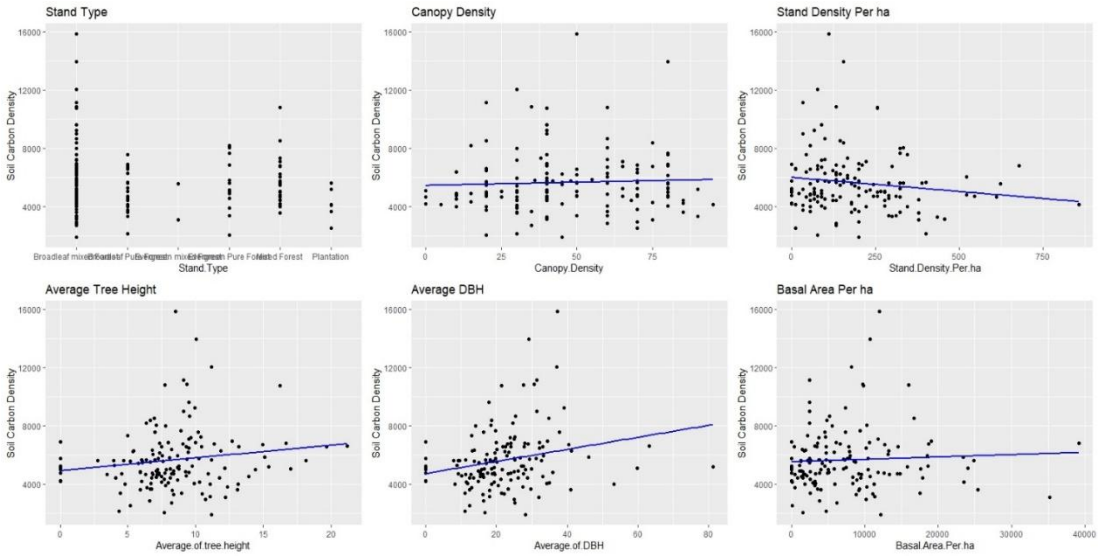

Figure 23. *Spearman correlation between stand structure and soil carbon density*

The model included diversity indices (Shannon-Wiener, Simpson's, and Pielou's Evenness) for species, diameter, and height classes, as well as stand characteristics like stand type, canopy density, stand density, average tree height, average DBH, and basal area. Stand type was treated as a categorical variable, while other predictors were modeled using smooth functions to capture non-linear effects. The GAM was fitted using the mgcv package in R, with carbon density as the dependent variable. The model formula included smooth terms for continuous predictors and parametric terms for categorical variables. Key findings from the model included: Parametric Coefficients: Stand types like Evergreen Pure Forest and Mixed Forest showed significant negative effects on carbon density, while other stand types were not significant. Smooth Terms: Significant non-linear relationships were observed for Simpson's Height Index, Pielou's Evenness Height, average tree height, and basal area. Basal area had the strongest influence, with a highly significant smooth term ($p < 2e^{-16}$).

The model explained 91.2% of the variability in carbon density (adjusted $R^2 = 0.912$) and 94.2% of the deviance, indicating a strong fit. The Generalized Cross-Validation (GCV) score of 6.7062e+07 and scale estimate of 4.4104e+07 suggested good predictive accuracy and model reliability (*Fig. 24*). Residual analysis and diagnostic plots were used to validate the model: Residuals: The mean residual was close to zero (-9.853563e-07), indicating minimal bias. However, the high standard deviation (5,410.12) suggested variability in prediction errors. Diagnostic Plots: Residuals were randomly scattered around zero, supporting the assumption of homoscedasticity. Smooth terms for predictors like basal area and average tree height showed significant non-linear relationships, while others, such as canopy density and stand density, had minimal impact.

http://www.aloki.hu ● ISSN 1589 1623 (Print) ● ISSN1785 0037 (Online)
DOI: http://dx.doi.org/10.15666/aeer/2305_85678605

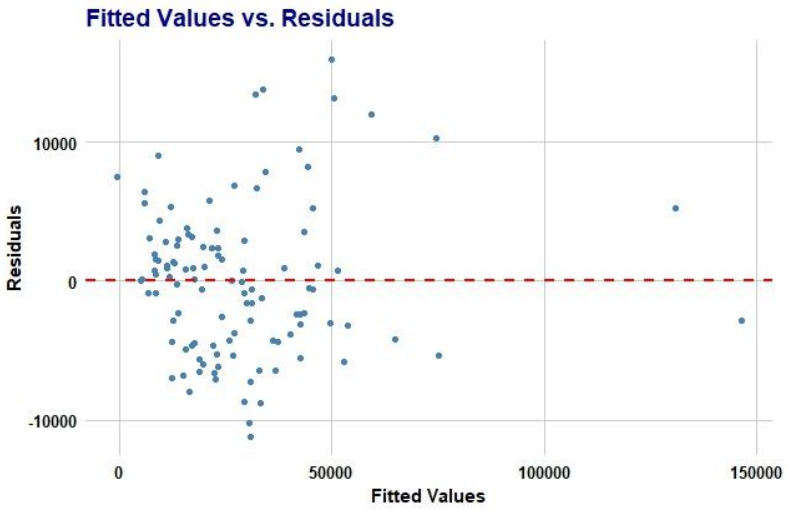

Figure 24. *Relationship between fitted values and residuals*

Model performance and predictive accuracy

The comparison between predicted and actual carbon density values reveals a strong correlation, with most data points closely aligned around the red line (*Fig. 25*). This close alignment indicates high predictive accuracy, consistent with the model's high R-squared value of 0.9417, which shows that the model explains 94.17% of the variance in carbon density (*Fig. 25*). While the majority of predictions are accurate, a few points deviate significantly, suggesting occasional prediction errors. Key performance metrics, including Mean Absolute Error (MAE = 4,195.54 kg/ha), Mean Squared Error (MSE = 29,005,671.08), and Root Mean Squared Error (RMSE = 5,385.69 kg/ha), further validate the model's accuracy. These metrics, though relatively high, are acceptable given the scale of the data and reflect the model's ability to provide reliable predictions.

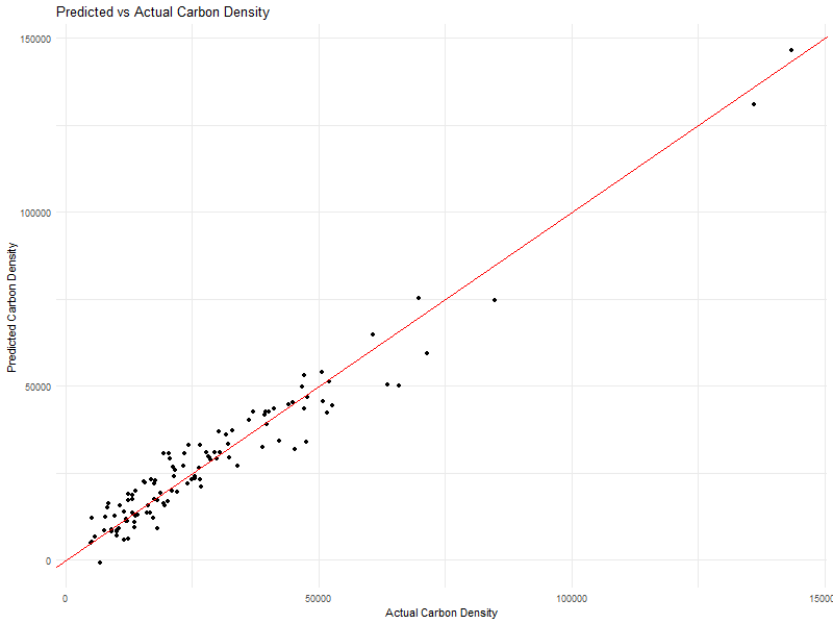

Figure 25. *Comparison of predicted and actual carbon density*

http://www.aloki.hu ● ISSN 1589 1623 (Print) ● ISSN1785 0037 (Online)
DOI: http://dx.doi.org/10.15666/aeer/2305_85678605

The observed and predicted carbon density values share the same mean (28,391.04 kg/ha), indicating that the model accurately captures the central tendency of the data (*Fig. 25*). However, the standard deviation of predicted values (21,483.24 kg/ha) is slightly lower than that of observed values (22,386.18 kg/ha), suggesting that the model smooths out some variability in the actual data (*Fig. 25*). Despite this, the high R^2 value and close alignment of means demonstrate the model's strong fit and predictive accuracy. The MAE, MSE, and RMSE values confirm reasonable prediction performance, with the model explaining a significant portion of the variance in carbon density. These results underscore the model's reliability for applications in forest management and carbon sequestration planning.

Discussion

Structural attributes of urban forest

Stand diversity

The analysis of species diversity in Beijing's urban forest reveals a high level of biodiversity, dominated by broad-leaved species (84%) over conifers (16%), with deciduous trees (75%) being more prevalent than evergreen species (25%). Families such as Rosaceae, Salicaceae, and Pinaceae are well-represented. Quantitative indices, including the Shannon-Wiener index (3.231), Simpson index (0.056), and Pielou's Evenness Index (0.7742), confirm high species diversity and evenness, indicating a balanced ecosystem. This diversity enhances resilience, carbon sequestration, and ecosystem services such as air purification and wildlife habitat provision. Previous studies, such as those by Alvey (2006) and Wang et al. (2024), support these findings, emphasizing the importance of species diversity in maintaining ecosystem stability and carbon sequestration potential.

At the plot level, species diversity varies significantly, with some plots showing near-complete dominance by a single species, while others exhibit high evenness. This heterogeneity suggests that local factors, such as habitat conditions and management practices, strongly influence species composition. The Importance Value Index (IVI) highlights the dominance of species like *Populus tomentosa* and *Sophora japonica*, which play critical roles in shaping forest structure and ecosystem dynamics. These findings underscore the need for targeted management strategies to enhance species richness and evenness in low-diversity plots, thereby improving urban forest quality and carbon sequestration potential. Moussa et al. (2020) found that urbanization in the Sahel alters urban forests, with Maradi having higher species richness and canopy cover than Niamey. Exotics made up 52% of species.

Diameter class diversity

The diameter class distribution in the urban forest shows moderate heterogeneity (Shannon-Wiener index = 2.32) and high evenness (Pielou's Evenness Index = 0.74, Simpson index = 0.88). This even distribution contrasts with the typical right-skewed distribution observed in many urban forests, suggesting a healthy and balanced age structure. The presence of trees across a wide range of diameter classes indicates successful management practices or favorable environmental conditions that support the growth of trees of varying sizes. This structural complexity enhances the forest's resilience and ability to withstand disturbances, making it a critical factor in urban forest

http://www.aloki.hu ● ISSN 1589 1623 (Print) ● ISSN1785 0037 (Online)
DOI: http://dx.doi.org/10.15666/aeer/2305_85678605

management. Similarly, a study on the diversity of street tree inventories across eight cities in the United States utilized the Simpson Index to assess species abundance and evenness, providing insights into the structural complexity of urban forests (Galle et al., 2021). Another study investigated the spatial pattern of tree diversity and evenness across forest types in Majella National Park, Italy, using Shannon diversity and evenness indices to explore variations in tree diversity (Redowan, 2015).

Height class diversity

Height class diversity analysis reveals a complex and balanced height structure, with moderate heterogeneity (Shannon-Wiener index = 2.09) and high evenness (Pielou's Evenness Index = 0.77, Simpson index = 0.85). The even distribution of height classes suggests a diverse age structure, which contributes to the forest's stability and ecological function. The presence of trees across multiple height classes enhances habitat heterogeneity, benefiting a wide range of fauna and fostering biodiversity. This balanced height distribution is essential for maintaining the forest's resilience and ability to provide ecosystem services. Additionally, research on the spatial patterns of tree diversity across different forest types in Majella National Park, Italy, utilized Shannon diversity and evenness indices to assess structural complexity. The study found that hop-hornbeam forests were the most diverse and even, while evergreen oak woods were the least, highlighting how structural diversity varies across forest types (Redowan, 2015).

Diversity complexity of height and diameter classes

The combined analysis of height and diameter class diversity highlights the urban forest's structural complexity. High evenness in diameter distribution (Pielou's Evenness Index = 0.917) and moderate heterogeneity (Shannon-Wiener index = 1.464) indicate a well-balanced representation of tree sizes. Similarly, height class diversity shows high evenness (Pielou's Evenness Index = 0.843) and moderate heterogeneity (Shannon-Wiener index = 1.060), suggesting a uniform vertical stratification. This structural diversity is crucial for habitat heterogeneity and ecosystem resilience, particularly in urban environments subject to anthropogenic pressures. Management practices should aim to maintain or enhance this diversity to promote long-term forest health and carbon sequestration.

Stand structure

The urban forest exhibits a moderately dense structure (181.60 trees/ha) with a high average basal area (7,305.78 m²/ha), indicating substantial biomass. However, significant variation in basal area across plots highlights heterogeneity within the forest. Dominant species such as Populus tomentosa, Sophora japonica, and Salix matsudana contribute disproportionately to basal area, suggesting a less diverse species composition than implied by the "Broadleaf Mixed Forest" designation. The diameter distribution shows a unimodal pattern, with 56% of trees in smaller diameter classes (<20 cm DBH) and only 15% in larger classes (>32 cm DBH), indicating a younger forest with ongoing regeneration. The height distribution is similarly skewed, with 70% of trees below 10 meters, further supporting the forest's relatively young age. These findings emphasize the need for integrated management strategies to promote a more balanced age and size class distribution, enhancing the forest's resilience and carbon sequestration potential. Similarly, height distribution in the Nigerian study showed a majority of trees below

http://www.aloki.hu ● ISSN 1589 1623 (Print) ● ISSN1785 0037 (Online)
DOI: http://dx.doi.org/10.15666/aeer/2305_85678605

10 meters, supporting the notion of relatively young urban forests (Dangulla et al., 2020). This observation is consistent with the current study, where 70% of trees were below 10 meters in height.

Biomass and soil carbon distribution

The urban forest stores a significant amount of carbon, with an average total biomass of 43,312.33 kg/ha. However, biomass distribution is uneven, with dominant species like *Populus tomentosa* contributing 26.81% of total biomass. The 20-39.9 cm diameter class accounts for approximately 50% of total biomass, highlighting the importance of mature trees in carbon storage. In contrast, smaller diameter classes (4-15.9 cm) contribute only 6%, indicating a potential deficiency in regeneration. Similarly, the 8-9.9 m height class represents 20.07% of total biomass, while smaller height classes (0-5.9 m) contribute only 4.43%, suggesting a bias towards middle-aged trees. Soil carbon density averages 5,666.17 kg/ha, with significant variability across plots, likely due to differences in soil properties and vegetation cover. These findings underscore the need for management strategies that promote species diversity, balanced age structures, and enhanced regeneration to improve carbon sequestration and ecosystem resilience. Comparatively, a national assessment of urban forest carbon storage in the United States estimated that urban forests with 28% canopy cover have, on average, about 52 trees per hectare, 60.5 metric tons of dry weight biomass per hectare, and a total of 27.2 metric tons of stored carbon per hectare. This suggests that the examined urban forest has a higher tree density but lower biomass and carbon storage per hectare than the national average (Rowntree and Nowak, 1991). Another study investigated the effects of urban forest types and traits on soil organic carbon sequestration, finding that forest types and traits substantially influence soil organic carbon stocks (Zhang et al., 2023; Yin et al., 2025). Diameter at breast height (DBH) was identified as a significant predictor variable, indicating that tree size and species composition are crucial factors in soil carbon sequestration (Xu et al., 2021).

Structural characteristics and total biomass correlation

Correlation and regression analyses reveal complex relationships between structural attributes and total biomass. A moderate negative correlation (-0.592) between diameter class and total biomass suggests that larger diameter classes, despite having higher individual biomass, contribute less to total biomass due to fewer trees. Similarly, a weak negative correlation (-0.326) between height class and total biomass indicates that taller trees do not significantly increase total biomass. These findings highlight the limitations of using diameter and height alone to predict biomass and emphasize the need for more comprehensive models that incorporate species composition, tree density, and environmental factors. Research indicates that larger diameter trees generally have access to better light conditions, which can enhance growth rates. However, despite their higher individual biomass, these trees may not significantly increase total biomass due to their lower numbers in the population. This aligns with the observed moderate negative correlation between diameter class and total biomass. Similarly, taller trees do not always correspond to higher total biomass, as evidenced by the weak negative correlation between height class and total biomass (Piponiot et al., 2022). These findings underscore the limitations of using diameter and height alone to predict biomass. Incorporating additional factors such as species composition, tree density, and environmental conditions into biomass models can enhance their accuracy. For instance, species-specific allometric

http://www.aloki.hu ● ISSN 1589 1623 (Print) ● ISSN1785 0037 (Online)
DOI: http://dx.doi.org/10.15666/aeer/2305_85678605

equations have been shown to provide more precise biomass estimates compared to generalized equations developed for traditional forests (McHale et al., 2009).

Impact assessment of stand attributes on biomass carbon density

Kruskal-Wallis and Spearman correlation analyses reveal that structural diversity, particularly in diameter and height classes, has a stronger influence on biomass carbon density than species diversity. Basal area ($r = 0.923$, $p < 0.0001$) and stand density ($r = 0.488$, $p < 0.0001$) show strong positive correlations with biomass carbon density, while canopy density ($r = 0.306$, $p < 0.0001$) and stand type ($r = -0.183$, $p = 0.023$) also play significant roles. These findings suggest that management practices should prioritize fostering structural diversity, such as maintaining a range of tree sizes and heights, to enhance carbon sequestration. Research indicates that structural diversity, particularly variations in tree diameter and height classes, significantly influences biomass carbon density in urban forests. For instance, a study in Changchun, Northeast China, utilized structural equation modeling to analyze the correlation between structural attributes and aboveground biomass (AGB) (Wu et al., 2022). The findings highlighted that both structural and species diversity attributes substantially affect AGB, emphasizing the role of structural complexity in carbon storage. Similarly, research in peri-urban areas revealed that denser stands with higher structural diversity hold greater carbon storage. The study found that stand basal area predominantly drives carbon storage, more so than tree density or species diversity (Balima et al., 2023). This underscores the importance of structural attributes in enhancing carbon sequestration. Moreover, a study in West Africa examined the impact of structural complexity and large-sized trees on aboveground carbon (AGC) relationships across various vegetation types. The research demonstrated that structural complexity and the presence of large trees play a significant role in explaining variations in AGC, further supporting the influence of structural attributes on biomass carbon density (Mensah et al., 2020).

Impact assessment of stand attributes on soil carbon density

Species diversity shows no significant relationship with soil carbon density, but diameter-based diversity, particularly Pielou's Evenness of diameter ($r = 0.20$, $p = 0.02$), exhibits a weak positive correlation. Average tree height ($r = 0.164$, $p = 0.047$) and average DBH ($r = 0.289$, $p = 0.0004$) also show significant positive correlations, indicating that larger trees contribute more to soil carbon density through increased litter input and root systems. These findings suggest that management practices promoting larger diameter trees may enhance soil carbon sequestration more effectively than increasing species richness alone. Ajid et al. (2025) studied the impact of stand density on soil organic carbon (SOC) stocks in Mongolian pine forests, finding that higher stand densities increased ecosystem carbon stocks but reduced mineral-associated organic carbon (MAOC) in the 0–10 cm soil layer. They emphasized the role of soil biochemical properties, such as microbial activity and litter quality, in mediating SOC dynamics (Zhang et al., 2025).

Modeling carbon density with generalized additive models

Generalized Additive Models (GAMs) were used to model carbon density, achieving an adjusted R-squared value of 0.912 and explaining 94.2% of the deviance. The model highlights the importance of tree height, basal area, and certain diversity indices (e.g.,

http://www.aloki.hu ● ISSN 1589 1623 (Print) ● ISSN1785 0037 (Online)
DOI: http://dx.doi.org/10.15666/aeer/2305_85678605

Simpson's Index for height) in predicting carbon density. Evergreen Pure Forest and Mixed Forest stand types show significantly lower carbon density compared to the baseline, while Broadleaf Pure Forest and Plantation types show no significant effects. The model's high predictive accuracy and strong performance make it a valuable tool for understanding and managing carbon dynamics in urban forests. Residual analysis confirms the model's reliability, with minor deviations from normality suggesting potential outliers. Overall, the GAM provides critical insights into the drivers of carbon density and offers a robust framework for future research and management strategies. Researchers have used GAM for various purposes. For example, Jiang et al. (2022) used a GAM to study TOC concentrations in the Danjiangkou Reservoir. The study found seasonal variations, with higher TOC in spring and summer, and spatial differences across the reservoir sites. Key factors influencing TOC included water temperature (WT), CODMn, ammonia nitrogen (NH_4^+-N), and total nitrogen (TN), with WT and Conductivity (Cond) showing linear relationships. De Brogniez et al. (2015) mapped topsoil organic carbon (OC) content across Europe using digital soil mapping and the LUCAS database. A GAM was applied, achieving an R^2 of 0.29. The model showed lower prediction accuracy for organic soils and in Scandinavia. The map revealed higher OC in wetlands, woodlands, and mountainous areas, while Mediterranean countries and croplands had lower OC content. The map also showed greater uncertainty in northern latitudes and wetlands. Steinparzer et al. (2025) applied GAM to study temperature regulation in a young experimental forest in Austria. They found that forests cool in summer and warm in winter, with species like Acer platanoides and Carpinus betulus showing the highest cooling effects. Mixed-species stands performed better than monocultures. Key factors influencing temperature regulation included solar radiation, humidity, and wind speed (Qi et al., 2023). Similarly, Koch et al. (2018) used GAM to model urban tree distributions for ash, maple, and oak trees, which are hosts for pests. They developed a three-step approach: estimating basal area (BA) proportions from street tree data, predicting BA for communities without inventories, and using GAM to estimate total BA based on canopy cover, location, and area. This approach provides more complete data for pest risk and spreads modeling.

Conclusions

The urban forest of Beijing exhibits high species and structural diversity, dominated by broadleaf and deciduous species. Key findings include high species richness (Shannon-Wiener index = 3.231) and evenness (Pielou's Evenness Index = 0.7742), contributing to ecosystem resilience and carbon sequestration. Structural heterogeneity is evident in the balanced distribution of diameter and height classes, with moderate heterogeneity (Shannon-Wiener index = 2.32 for diameter, 2.09 for height) and high evenness (Pielou's Evenness Index = 0.74 for diameter, 0.77 for height), indicating a healthy and resilient forest structure. Biomass distribution analysis reveals that dominant species like *Populus tomentosa* contribute significantly to total biomass (26.81%), with the 20-39.9 cm diameter class accounting for 50% of total biomass. However, smaller diameter (4-15.9 cm) and height (0-5.9 m) classes are underrepresented, highlighting a need for improved regeneration strategies.

Structural diversity, particularly in diameter and height classes, strongly influences biomass carbon density. Basal area ($r = 0.923$, $p < 0.0001$) and stand density ($r = 0.488$, $p < 0.0001$) are key predictors of carbon storage, emphasizing the importance of

http://www.aloki.hu ● ISSN 1589 1623 (Print) ● ISSN1785 0037 (Online)
DOI: http://dx.doi.org/10.15666/aeer/2305_85678605

maintaining a diverse and balanced tree structure. Soil carbon density is positively correlated with average tree height ($r = 0.164$, $p = 0.047$) and average DBH ($r = 0.289$, $p = 0.0004$), underscoring the role of larger trees in enhancing soil carbon storage through increased litter input and root systems. These findings suggest that management practices promoting larger diameter trees may enhance soil carbon sequestration more effectively than simply increasing species richness.

The application of Generalized Additive Models (GAMs) successfully captured the complex, non-linear relationships between structural attributes and carbon density, achieving high predictive accuracy (adjusted $R^2 = 0.912$, deviance explained = 94.2%). This modeling approach provides a robust framework for predicting carbon density and informing urban forest management strategies. In conclusion, this study highlights the importance of structural diversity and targeted management practices, such as promoting larger diameter trees and balanced age structures, to enhance carbon sequestration and ecosystem resilience. Urban forest management should consider holistic structural features to optimize carbon storage and mitigate climate change. The successful application of GAMs offers a reliable tool for predicting carbon density and guiding future urban forest conservation and planning efforts.

Conflict of interests. The authors declare no conflict of interests.

Funding. This work was supported by the National Key Research and Development Program of China: Green Urbanization across China and Europe: Collaborative Research on Key Technological Advances in Urban Forests [grant number 2021YFE0193200-3], National Natural Science Foundation of China (32271832) and 5·5 Engineering Research & Innovation Team Project of Beijing Forestry University (No: BLRC2023B06).

REFERENCES

[1] Alvey, A. A. (2006): Promoting and preserving biodiversity in the urban forest. – Urban For Urban Green 5: 195-201. https://doi.org/10.1016/j.ufug.2006.09.003.

[2] Balima, L. H., Zerbo, I., Bayen, P., Kiemtoré, H., Ganamé, M., Cissé, M., Thiombiano, A. (2023): Higher diversity, denser stands and greater biomass in peri-urban forests than in adjacent agroforestry systems in Western Burkina Faso: implications for urban sustainability. – Environ Monit Assess 195: 1077. https://doi.org/10.1007/s10661-023-11707-7.

[3] Bhuyan, P. (2003): Tree diversity and population structure in undisturbed and human-impacted stands of tropical wet evergreen forest in Arunachal Pradesh, Eastern Himalayas, India. – Biodivers Conserv 12: 1753-1773. https://doi.org/10.1023/A:1023619017786.

[4] Bottalico, F., Chirici, G., Giannetti, F., De Marco, A., Nocentini, S., Paoletti, E., Salbitano, F., Sanesi, G., Serenelli, C., Travaglini, D. (2016): Air Pollution Removal by Green Infrastructures and Urban Forests in the City of Florence. – Agriculture and Agricultural Science Procedia 8: 243-251. https://doi.org/10.1016/j.aaspro.2016.02.099.

[5] Brom, P., Engemann, K., Breed, C., Pasgaard, M., Onaolapo, T., Svenning, J.-C. (2023): A Decision Support Tool for Green Infrastructure Planning in the Face of Rapid Urbanization. – Land (Basel) 12: 415. https://doi.org/10.3390/land12020415.

[6] Chen, B., Qi, X., Qiu, Z. (2018): Recreational use of urban forest parks: a case study in Fuzhou National Forest Park, China. – Journal of Forest Research 23: 183-189. https://doi.org/10.1080/13416979.2018.1432304.

[7] Chen, W. Y., Li, X. (2021): Urban forests' recreation and habitat potentials in China: A nationwide synthesis. – Urban For Urban Green 66: 127376.

http://www.aloki.hu ● ISSN 1589 1623 (Print) ● ISSN1785 0037 (Online)
DOI: http://dx.doi.org/10.15666/aeer/2305_85678605

https://doi.org/10.1016/j.ufug.2021.127376.

[8] Dangulla, M., Abd Manaf, L., Ramli, M. F., Yacob, M. R. (2020): Urban tree composition, diversity and structural characteristics in North-western Nigeria. – Urban For Urban Green 48: 126512. https://doi.org/10.1016/j.ufug.2019.126512.

[9] de Brogniez, D., Ballabio, C., Stevens, A., Jones, R. J. A., Montanarella, L., van Wesemael, B. (2015): A map of the topsoil organic carbon content of Europe generated by a generalized additive model. – Eur J Soil Sci 66: 121-134. https://doi.org/10.1111/ejss.12193.

[10] Du, C., Bai, X., Li, Y., Tan, Q., Zhao, C., Luo, G., Wang, J., Wu, L., Li, C., Li, J., Xie, Y., Ran, C., Zhang, S., Xiong, L., Yuang, X., Liao, J., Dai, L., Long, M., Li, Z., Xue, Y., Zhang, X., Luo, Q., Shen, X., Yang, S., Li, M. (2024): The restoration of karst rocky desertification has enhanced the carbon sequestration capacity of the ecosystem in southern China. – Glob Planet Change 243: 104602. https://doi.org/10.1016/j.gloplacha.2024.104602.

[11] Escobedo, F. J., Wagner, J. E., Nowak, D. J., De la Maza, C. L., Rodriguez, M., Crane, D. E. (2008) Analyzing the cost effectiveness of Santiago, Chile's policy of using urban forests to improve air quality. – J Environ Manage 86: 148-157. https://doi.org/10.1016/j.jenvman.2006.11.029.

[12] Feng, Y., Chen, J., Luo, J. (2024): Life cycle cost analysis of power generation from underground coal gasification with carbon capture and storage (CCS) to measure the economic feasibility. – Resources Policy 92: 104996. https://doi.org/10.1016/j.resourpol.2024.104996.

[13] Galle, N. J., Halpern, D., Nitoslawski, S., Duarte, F., Ratti, C., Pilla, F. (2021): Mapping the diversity of street tree inventories across eight cities internationally using open data. – Urban For Urban Green 61: 127099. https://doi.org/10.1016/j.ufug.2021.127099.

[14] Ganesh, K. P., Pragasan, L. A. (2022): Effects of nitrogen addition on *Eucalyptus globulus* growth and carbon sequestration potential under various CO_2 climatic conditions. – Geology, Ecology, and Landscapes 8: 185-193. https://doi.org/10.1080/24749508.2022.2109834.

[15] Gelan, E., Girma, Y. (2021): Sustainable Urban Green Infrastructure Development and Management System in Rapidly Urbanized Cities of Ethiopia. – Technologies (Basel) 9: 66. https://doi.org/10.3390/technologies9030066.

[16] Georgi, N. J., Zafiriadis, K. (2006): The impact of park trees on microclimate in urban areas. – Urban Ecosyst 9: 195-209. https://doi.org/10.1007/s11252-006-8590-9.

[17] Giraldo-Charria, D. L., Escobedo, F. J., Clerici, N., Quesada, B. (2025): Urban forests mitigate extreme heat exposure in a vulnerable tropical city. – Urban Clim 59: 102311. https://doi.org/10.1016/j.uclim.2025.102311.

[18] Guo, Y., Ren, Z., Wang, C., Zhang, P., Ma, Z., Hong, S., Hong, W., He, X. (2024): Spatiotemporal patterns of urban forest carbon sequestration capacity: Implications for urban CO_2 emission mitigation during China's rapid urbanization. – Science of The Total Environment 912: 168781. https://doi.org/10.1016/j.scitotenv.2023.168781.

[19] He, C., Liu, Z., Wu, J., Pan, X., Fang, Z., Li, J., Bryan, B. A. (2021): Future global urban water scarcity and potential solutions. – Nat Commun 12: 4667. https://doi.org/10.1038/s41467-021-25026-3.

[20] He, Q., Zhan, J., Liu, X., Dong, C., Tian, D., Fu, Q. (2025): Multispectral polarimetric bidirectional reflectance research of plant canopy. – Opt Lasers Eng 184: 108688. https://doi.org/10.1016/j.optlaseng.2024.108688.

[21] IPCC (2006): IPCC guidelines for national greenhouse gas inventories. – Intergovernmental Panel on Climate Change, Task Force on National Greenhouse Gas Inventories.

[22] Jiang, Y., He, K., Li, Y., Qin, M., Cui, Z., Zhang, Y., Yao, Y., Chen, X., Deng, M., Gray, A., Li, B. (2022): Driving Factors of Total Organic Carbon in Danjiangkou Reservoir Using Generalized Additive Model. – Water (Basel) 14: 891. https://doi.org/10.3390/w14060891.

http://www.aloki.hu ● ISSN 1589 1623 (Print) ● ISSN1785 0037 (Online)
DOI: http://dx.doi.org/10.15666/aeer/2305_85678605

[23] Koch, F. H., Ambrose, M. J., Yemshanov, D., Wiseman, P. E., Cowett, F. D. (2018): Modeling urban distributions of host trees for invasive forest insects in the eastern and central USA: A three-step approach using field inventory data. – For Ecol Manage 417: 222-236. https://doi.org/10.1016/j.foreco.2018.03.004.

[24] Li, T., & Li. Y., (2023): Artificial intelligence for reducing the carbon emissions of 5G networks in China. – Nat Sustain 6: 1522-1523. https://doi.org/10.1038/s41893-023-01208-3.

[25] Li, T., Xin, S., Xi, Y., Tarkoma, S., Hui, P., Li, Y. (2022). Predicting Multi-level Socioeconomic Indicators from Structural Urban Imagery. Paper presented at the CIKM '22: Proceedings of the 31st ACM International Conference on Information & Knowledge Management, New York, NY, USA. https://doi.org/10.1145/3511808.3557153

[26] Luo, Y., Wang, X., Ouyang, Z., Lu, F., Feng, L., Tao, J. (2018): A China's normalized tree biomass equation dataset. – Earth Syst. Sci. Data Discuss.

[27] Mao, Q., Huang, G., Buyantuev, A., Wu, J., Luo, S., Ma, K. (2014): Spatial heterogeneity of urban soils: the case of the Beijing metropolitan region, China. – Ecol Process 3: 23. https://doi.org/10.1186/s13717-014-0023-8.

[28] McHale, M. R., Burke, I. C., Lefsky, M. A., Peper, P. J., McPherson, E. G. (2009): Urban forest biomass estimates: is it important to use allometric relationships developed specifically for urban trees? – Urban Ecosyst 12: 95-113. https://doi.org/10.1007/s11252-009-0081-3.

[29] Mensah, S., Salako, V. K., Seifert, T. (2020): Structural complexity and large-sized trees explain shifting species richness and carbon relationship across vegetation types. – Funct Ecol 34: 1731-1745. https://doi.org/10.1111/1365-2435.13585.

[30] Morgenroth, J., Nowak, D., Koeser, A. (2020): DBH Distributions in America's Urban Forests: An Overview of Structural Diversity. – Forests 11: 135. https://doi.org/10.3390/f11020135.

[31] Moussa, S., Kuyah, S., Kyereh, B., Tougiani, A., Mahamane, S. (2020): Diversity and structure of urban forests of Sahel cities in Niger. – Urban Ecosyst 23: 851-864. https://doi.org/10.1007/s11252-020-00984-6.

[32] Nowak, D. J., Hirabayashi, S., Doyle, M., McGovern, M., Pasher, J. (2018): Air pollution removal by urban forests in Canada and its effect on air quality and human health. – Urban For Urban Green 29: 40-48. https://doi.org/10.1016/j.ufug.2017.10.019.

[33] Oberle, B., Bressan, S., McWilliams, J., Díaz-Almeyda, E. (2023): Urban food forestry transforms fine-scale soil function for rapid and uniform carbon sequestration. – Urban Ecosyst 26: 1239-1250. https://doi.org/10.1007/s11252-023-01384-2.

[34] Obonyo, O. A., Agevi, H., Tsingalia, M. H. (2023): Above-ground carbon stocks and its functional relationship with tree species diversity: the case of Kakamega and North Nandi Forests, Kenya. – Sci Rep 13: 20921. https://doi.org/10.1038/s41598-023-47871-6.

[35] Piponiot, C., Anderson-Teixeira, K. J., Davies, S. J., Allen, D., Bourg, N. A., Burslem, D. F. R. P., Cárdenas, D., Chang-Yang, C., Chuyong, G., Cordell, S., Dattaraja, H. S., Duque, Á., Ediriweera, S., Ewango, C., Ezedin, Z., Filip, J., Giardina, C. P., Howe, R., Hsieh, C., Hubbell, S. P., Inman-Narahari, F. M., Itoh, A., Janík, D., Kenfack, D., Král, K., Lutz, J. A., Makana, J., McMahon, S. M., McShea, W., Mi, X., Bt. Mohamad, M., Novotný, V., O'Brien, M. J., Ostertag, R., Parker, G., Pérez, R., Ren, H., Reynolds, G., Md Sabri, M. D., Sack, L., Shringi, A., Su, S., Sukumar, R., Sun, I., Suresh, H. S., Thomas, D. W., Thompson, J., Uriarte, M., Vandermeer, J., Wang, Y., Ware, I. M., Weiblen, G. D., Whitfeld, T. J. S., Wolf, A., Yao, T. L., Yu, M., Yuan, Z., Zimmerman, J. K., Zuleta, D., Muller-Landau, H. C. (2022): Distribution of biomass dynamics in relation to tree size in forests across the world. – New Phytologist 234: 1664-1677. https://doi.org/10.1111/nph.17995.

[36] Qi, X., Qian, S., Chen, K., Li, J., Wu, X., Wang, Z., Deng, Z., Jiang, J. (2023): Dependence of daily precipitation and wind speed over coastal areas: evidence from China's coastline. – Hydrology Research 54: 491-507. https://doi.org/10.2166/nh.2023.093.

http://www.aloki.hu ● ISSN 1589 1623 (Print) ● ISSN1785 0037 (Online)
DOI: http://dx.doi.org/10.15666/aeer/2305_85678605

[37] Qiu, S., Yang, H., Zhang, S., Huang, S., Zhao, S., Xu, X., He, P., Zhou, W., Zhao, Y., Yan, N., Nikolaidis, N., Christie, P., Banwart, S. A. (2023): Carbon storage in an arable soil combining field measurements, aggregate turnover modeling and climate scenarios. – Catena (Amst) 220: 106708. https://doi.org/10.1016/j.catena.2022.106708.
[38] Redowan, M. (2015): Spatial pattern of tree diversity and evenness across forest types in Majella National Park, Italy. – For Ecosyst 2: 24. https://doi.org/10.1186/s40663-015-0048-1.
[39] Rowntree, R., Nowak, D. (1991): Quantifying the Role of Urban Forests in Removing Atmospheric Carbon Dioxide. – Arboric Urban For 17: 269-275. https://doi.org/10.48044/jauf.1991.061.
[40] Sarkodie, S. A., Owusu, P. A., Leirvik, T. (2020): Global effect of urban sprawl, industrialization, trade and economic development on carbon dioxide emissions. – Environmental Research Letters 15: 034049. https://doi.org/10.1088/1748-9326/ab7640.
[41] Scholz, T., Hof, A., Schmitt, T. (2018): Cooling Effects and Regulating Ecosystem Services Provided by Urban Trees: Novel Analysis Approaches Using Urban Tree Cadastre Data. – Sustainability 10: 712. https://doi.org/10.3390/su10030712.
[42] Shadman, S., Ahanaf Khalid, P., Hanafiah, M. M., Koyande, A. K., Islam, Md. A., Bhuiyan, S. A., Sin Woon, K., Show, P.-L. (2022): The carbon sequestration potential of urban public parks of densely populated cities to improve environmental sustainability. – Sustainable Energy Technologies and Assessments 52: 102064. https://doi.org/10.1016/j.seta.2022.102064.
[43] Steinparzer, M., Gillerot, L., Rewald, B., Godbold, D. L., Haluza, D., Guo, Q., Vospernik, S. (2025): Forest temperature buffering in pure and mixed stands: A high-resolution temporal analysis with generalized additive models. – For Ecol Manage 583: 122582. https://doi.org/10.1016/j.foreco.2025.122582.
[44] Sun, Y., Xie, S., Zhao, S. (2019): Valuing urban green spaces in mitigating climate change: A city-wide estimate of aboveground carbon stored in urban green spaces of China's Capital. – Glob Chang Biol 25: 1717-1732. https://doi.org/10.1111/gcb.14566.
[45] Sun, B., Xu, Z., Wei, M., Wang, X. (2025): A study on the strategic behavior of players participating in air-rail intermodal transportation based on evolutionary games. – J Air Transp Manag 126: 102793. https://doi.org/10.1016/j.jairtraman.2025.102793.
[46] Ullah, S., Abbas, M., Qiao, X. (2024a): Impact assessment of land-use alteration on land surface temperature in Kabul using machine learning algorithm. – J Spat Sci 70(1): 1-23. https://doi.org/10.1080/14498596.2024.2364283.
[47] Ullah, S., Khan, M., Qiao, X. (2024b): Examining the impact of land use and land cover changes on land surface temperature in Herat city using machine learning algorithms. – GeoJournal 89: 225. https://doi.org/10.1007/s10708-024-11217-0.
[48] Ullah, S., Qiao, X., Abbas, M. (2024c): Addressing the impact of land use land cover changes on land surface temperature using machine learning algorithms. – Sci Rep 14: 18746. https://doi.org/10.1038/s41598-024-68492-7.
[49] Ullah, S., Khan, M., Qiao, X. (2025a): Evaluating the impact of urbanization patterns on LST and UHI effect in Afghanistan's Cities: a machine learning approach for sustainable urban planning. – Environ Dev Sustain. https://doi.org/10.1007/s10668-025-06249-6.
[50] Ullah, S., Qiao, X., Tariq, A. (2025b): Impact assessment of planned and unplanned urbanization on land surface temperature in Afghanistan using machine learning algorithms: a path toward sustainability. – Sci Rep 15: 3092. https://doi.org/10.1038/s41598-025-87234-x.
[51] Vogt, J., Gillner, S., Hofmann, M., Tharang, A., Dettmann, S., Gerstenberg, T., Schmidt, C., Gebauer, H., Van de Riet, K., Berger, U., Roloff, A. (2017): Citree: A database supporting tree selection for urban areas in temperate climate. – Landsc Urban Plan 157: 14-25. https://doi.org/10.1016/j.landurbplan.2016.06.005.
[52] Wang, K., She, D., Zhang, X., Wang, Y., Wen, H., Yu, J., Wang, Q., Han, S., Wang, W. (2024): Tree richness increased biomass carbon sequestration and ecosystem stability of

http://www.aloki.hu ● ISSN 1589 1623 (Print) ● ISSN1785 0037 (Online)
DOI: http://dx.doi.org/10.15666/aeer/2305_85678605

temperate forests in China: Interacted factors and implications. – J Environ Manage 368: 122214. https://doi.org/10.1016/j.jenvman.2024.122214.

[53] Wu, J., Wang, Z., Zhang, D., Gong, C., Zhai, C., Wang, Y. (2022): Effects of Structural and Diversity Attributes on Biomass in Different Types of Urban Forests in Changchun, Northeast China, and Suggestions for Urban Forest Planning. – Forests 13: 1805. https://doi.org/10.3390/f13111805.

[54] Wu, C., Wang, R., Lu, S., Tian, J., Yin, L., Wang, L., Zheng, W. (2025a): Time-Series Data-Driven PM2.5 Forecasting: From Theoretical Framework to Empirical Analysis. – Atmosphere (Basel) 16: 292. https://doi.org/10.3390/atmos16030292.

[55] Wu, L., Bai, X., Li, C., Li, H., Cao, Y., Ran, C., Zhang, S., Xiong, L., Du, C., Luo, G., Chen, F., Wei, H., Chen, D., Yang, D., Xiong, L., Jia, J. (2025b): Assessment of carbon sinks caused by the chemical weathering of carbonate rocks under the influence of exogenous acids: Methods, progress, and prospects. – Sci China Earth Sci 68: 1785-1804. https://doi.org/10.1007/s11430-024-1549-y.

[56] Xu, X., Sun, Z., Hao, Z., Bian, Q., Wei, K., Wang, C. (2021): Effects of Urban Forest Types and Traits on Soil Organic Carbon Stock in Beijing. – Forests 12: 394. https://doi.org/10.3390/f12040394.

[57] Yan, J., Zhou, W., Zheng, Z., Wang, J., Tian, Y. (2020): Characterizing variations of greenspace landscapes in relation to neighborhood characteristics in urban residential area of Beijing, China. – Landsc Ecol 35: 203-222. https://doi.org/10.1007/s10980-019-00943-3.

[58] Yang, Y., Lv, Y., Zhou, D. (2025): The impact of urban parks on the thermal environment of built-up areas and an optimization method. – PLoS One 20: e0318633. https://doi.org/10.1371/journal.pone.0318633.

[59] Yin, Y., Gong, H., Chen, Z., Tian, X., Wang, Y., Wang, Z., He, K., Miao, Q., Chu, Y., Xue, Y., Zhang, Q., Cui, Z. (2025): Underestimated sequestration of soil organic carbon in China. – Environ Chem Lett 23: 373-379. https://doi.org/10.1007/s10311-024-01813-4.

[60] Zhao, Y., Yingrui, G., Moru, L., Zhifeng, Z., & Pengjun, Z. (2025a). Mobility constraints of residents in marginal rural areas of megacities: Evidence from Beijing, China. – J Transp Geogr 127: 104259. https://doi.org/10.1016/j.jtrangeo.2025.104259.

[61] Zhang, T., Song, B., Han, G., Zhao, H., Hu, Q., Zhao, Y., Liu, H. (2023): Effects of coastal wetland reclamation on soil organic carbon, total nitrogen, and total phosphorus in China: A meta-analysis. – Land Degrad Dev 34: 3340-3349. https://doi.org/10.1002/ldr.4687.

[62] Zhang, B. (2025): Perceptions of trade-offs between urban forest ecosystem services and disservices: A case study of Canberra, Australia. – Urban For Urban Green 105: 128711. https://doi.org/10.1016/j.ufug.2025.128711.

[63] Zhang, Y., Zeng, D.-H., Sheng, Z., Wang, Q.-W., Yu, D., Lin, G. (2025): Stand density influences soil organic carbon stocks and fractions by mediating soil biochemical properties in Mongolian pine plantations. – Plant Soil. https://doi.org/10.1007/s11104-025-07317-6.

[64] Zhao, Y., Ma, J., Li, Y., Cheng, K., Zhang, M., Liu, Z., Yang, F. (2025b): Carbon Emission Based Predictions of Anthropogenic Impacts on Groundwater Storage at Typical Basins in 2050. – Research 8. https://doi.org/10.34133/research.0680.

[65] Zürcher, N., Andreucci, M.-B. (2017): Growing the Urban Forest: Our Practitioners' Perspective. – In: Pearlmutter, D. (ed.) The Urban Forest, pp. 315-346. https://doi.org/10.1007/978-3-319-50280-9_24.

http://www.aloki.hu ● ISSN 1589 1623 (Print) ● ISSN1785 0037 (Online)
DOI: http://dx.doi.org/10.15666/aeer/2305_85678605